# Study of the Chemistry of *ortho*- and *para*-Biphenylnitrenes by Laser Flash Photolysis and Time-Resolved IR Experiments and by B3LYP and CASPT2 Calculations

Meng-Lin Tsao,[†] Nina Gritsan,*,[‡] Tammi R. James,[†] Matthew S. Platz,*,[†]
David A. Hrovat,[§] and Weston Thatcher Borden*,[§]

*Contribution from the Department of Chemistry, The Ohio State University,
Columbus, Ohio 43210, Institute of Chemical Kinetics and Combustion and
Novosibirsk State University, 630090 Novosibirsk, Russia, and Department of Chemistry,
Box 351700, University of Washington, Seattle, Washington 98195-1700*

Received March 14, 2003;  E-mail: platz.1@osu.edu

**Abstract:** The photochemistry of *ortho*-biphenyl azide (**1a**) has been studied by laser flash photolysis (LFP), with UV–vis and IR detection of the transient intermediates formed. LFP (266 nm) of **1a** in glassy 3-methylpentane at 77 K releases singlet *ortho*-biphenylnitrene (**1b**) ($\lambda_{max} = 410$ nm, $\tau = 59 \pm 6$ ns), which under these conditions decays cleanly to the lower energy triplet state. In fluid solution at 298 K, **1b** rapidly ($\tau < 10$ ns) partitions between formation of isocarbazole (**4**) ($\lambda_{max} = 430$ nm, $\tau = 70$ ns) and benzazirine (**1e**) ($\lambda_{max} = 305$ nm, $\tau = 12$ ns). Isocarbazole **4** undergoes a 1,5-hydrogen shift, with $k_H/k_D = 3.4$ at 298 K to form carbazole **9** and smaller amounts of two other isocarbazoles (**7** and **8**). Benzazirine **1e** ring-opens reversibly to azacycloheptatetraene (**1f**), which serves as a reservoir for singlet nitrene **1b**. Azacycloheptatetraene **1f** ultimately forms carbazole **9** on the millisecond time scale by the pathway **1f** → **1e** → **1b** → **4** → **9**. The energies of the transient intermediates and of the transition structures connecting them were successfully predicted by CASPT2/6-31G* calculations. The electronic and vibrational spectra of the intermediates, computed by density functional theory, support the assignment of the transient spectra, observed in the formation of **9** from **1a**.

## I. Introduction

In 1951, Smith and Brown reported that carbazole **9** was formed upon pyrolysis of *ortho*-biphenyl azide (**1a**).[1]
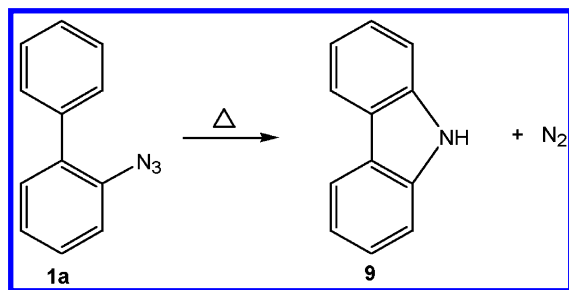


This reaction has fascinated chemists ever since its discovery, because it is one of the few synthetically useful reactions of simple aryl azides.[2]

Nitrogen loss from **1a** can be initiated photochemically, which has led to studies of the reactive intermediates involved in the

transformation of **1a** to **9** by chemical trapping,[3] matrix spectroscopy,[4] and flash photolysis.[3c,5] Swenton, Ikeler, and Williams[6] demonstrated that carbazole is derived from the reaction of a singlet state species, presumably singlet nitrene **1b**, whereas triplet nitrene **1c** dimerizes to form azo compound **1d** (Scheme 1).

Berry[5] and Sundberg[3c] studied the formation of **9** from **1a** by monitoring the change in carbazole absorption at its maximum (289.4 nm). Carbazole was formed in cyclohexane with a rate constant of $2.2 \times 10^3$ s$^{-1}$ at 300 K by passage over a reaction barrier of 11.5 kcal/mol.[5] Sundberg et al.[3c] obtained similar results in other hydrocarbon solutions, but they found that the rate constant of carbazole formation is solvent dependent and increases to $\sim 2 \times 10^4$ s$^{-1}$ in methanol. Because the rate constant ($k_c$) for cyclization of singlet phenylnitrene (**2b** in Scheme 2) is 5–6 orders of magnitude greater than these values,[7–9] it seems unlikely that these values are actually the

[†] The Ohio State University.
[‡] Novosibirsk State University.
[§] University of Washington.

(1) (a) Smith, P. A. S.; Brown, B. B. *J. Am. Chem. Soc.* **1951**, *73*, 2438. (b) Smith, P. A. S.; Brown, B. B. *J. Am. Chem. Soc.* **1951**, *73*, 2435. (c) Smith, P. A. S.; Hall, J. H. *J. Am. Chem. Soc.* **1962**, *84*, 1632.
(2) (a) Smith, P. A. S. In *Azides and Nitrenes*; Scriven, E. F. U., Ed.; Academic Press: New York, 1984; p 95. (b) Walker, P.; Waters, W. A. *J. Am. Chem. Soc.* **1961**, *83*, 408.

(3) (a) Sundberg, R. J.; Brenner, M.; Suter, S. R.; Das, B. P. *Tetrahedron Lett.* **1970**, *31*, 2715. (b) Sundberg, R. J.; Heintzelman, R. W. *J. Org. Chem.* **1974**, *39*, 2546. (c) Sundberg, R. J.; Gillespie, D. W.; DeGraff, B. A. *J. Am. Chem. Soc.* **1975**, *97*, 6193.
(4) (a) Reiser, A.; Wanger, H.; Bowes, G. *Tetrahedron Lett.* **1966**, *23*, 629. (b) Reiser, A.; Willets, F. W.; Terry, G. C.; Williams, V.; Marley, R. *Trans. Faraday Soc.* **1968**, *4*, 3265. (c) Reiser, A.; Bowes, G.; Horne, R. J. *Trans. Faraday Soc.* **1966**, *62*, 3162.
(5) Lehman, P. A.; Berry, R. S. *J. Am. Chem. Soc.* **1973**, *95*, 8614.
(6) Swenton, J.; Ikeler, T.; Williams, B. *J. Am. Chem. Soc.* **1970**, *92*, 3103.
(7) Gritsan, N. P.; Yuzawa, T.; Platz, M. S. *J. Am. Chem. Soc.* **1997**, *119*, 5059.
(8) Born, R.; Burda, C.; Senn, P.; Wirz, J. *J. Am. Chem. Soc.* **1997**, *119*, 5062.

*Scheme 1*
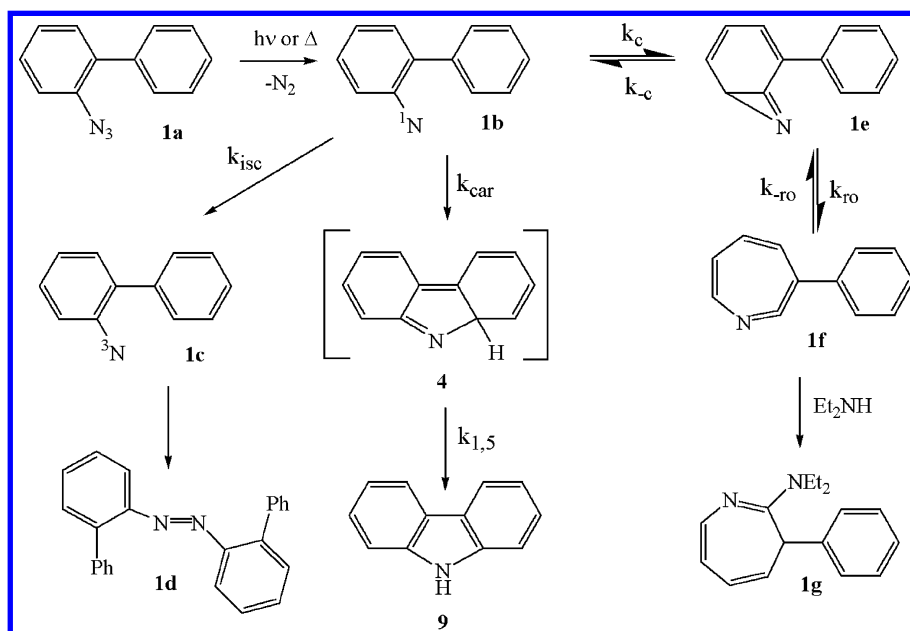


*Scheme 2*
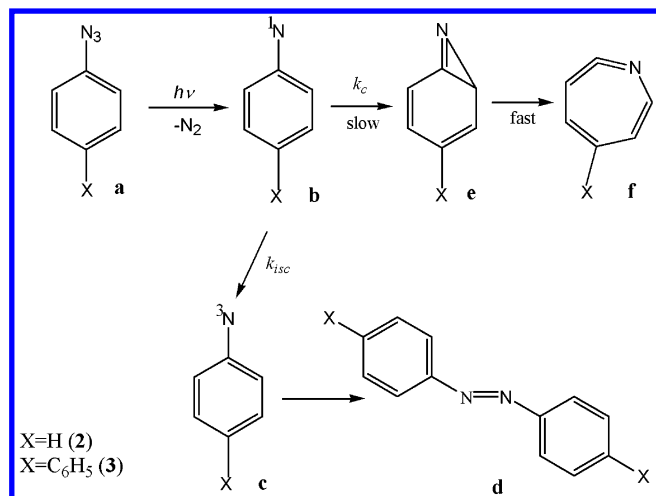


rate constants for formation of **9** in a simple one-step mechanism from singlet *ortho*-biphenylnitrene (**1b**).

Indeed, the Sundberg group[3a,b] demonstrated that, in the presence of diethylamine, photolysis of azide **1a** leads to the formation of azepine **1g** (Scheme 1), with a concomitant reduction in the yield of carbazole. Sundberg et al.[3] concluded that diethylamine traps azirine **1e** and that some **1e** must revert to singlet nitrene **1b**, to explain the reduction in the yield of **9**. Other groups have argued that azacycloheptatetraene (**1f**) is the amine-trappable species, and this hypothesis requires that the formation of both **1e** and **1f** from **1b** be reversible.

Although the Sundberg group[3a,b] discovered that increasing concentrations of diethylamine reduced the formation of carbazole, even the highest amine concentrations reduced the yield of **9** by only about 50%. This finding suggests that $k_{car}$ is comparable in size to $k_c$ (Scheme 1), so that singlet *ortho*-biphenylnitrene (**1b**), produced by photolysis of **1a**, partitions about equally between formation of carbazole **9** and azirine **1e**.

(9) Gritsan, N. P.; Zhu, Z.; Hadad, C. M.; Platz, M. S. *J. Am. Chem. Soc.* **1999**, *121*, 1202.

Approximately equal partitioning of **1b** would explain why the yield of **9** is reduced by only a factor of 2, even if all of the **1e** that is generated is trapped as the diethylamine adduct (**1g**) of azacycloheptatetraene (**1f**).

The mechanism of carbazole formation, shown in Scheme 1, was first proposed in 1992.[10,11] It was based on studies of the photochemistry of **1a**[3-6] and on the time-resolved (TR)IR data of Schuster et al. on the intermediates formed by photolysis of phenyl azide **2a** and some of its simple derivatives.[12]

More recently, we have used laser flash photolysis techniques to observe directly singlet phenylnitrene ($\lambda_{max}$ = 335 and 352 nm) and to measure its rate of cyclization ($k_c \approx 10^9$ s$^{-1}$) to benzazirine **2e** (Scheme 2).[7-9] The successful observation of **2b** led us to study the photochemistry of *ortho*- and *para*-biphenyl azides (**1a** and **3a**) by time-resolved spectroscopy. We hoped to observe and identify the transient intermediates involved in the formation of carbazole **9**. Herein, we are pleased to report our results.

## II. Results

**II.1. Calculations.** Given the previous successes of electronic structure calculations in explaining and predicting the chemistry of phenylnitrene (**2b**) and derivatives,[13] we performed calculations of the potential energy surface for the possible rearrangements of *ortho*-biphenylnitrene (**1b**), concurrently with carrying out time-resolved spectroscopic measurements. The results of our calculations are described in this section, and the results of our experimental studies are described in Section II.2.

(10) Schuster, G. B.; Platz, M. S. *Adv. Photochem.* **1992**, *17*, 69.
(11) Gritsan, N. P.; Pritchina, E. A. *Russ. Chem. Rev.* **1992**, *61*, 500.
(12) (a) Shields, C. J.; Chrisope, D. R.; Schuster, G. B.; Dixon, A. J.; Poliakoff, M.; Turner, J. J. *J. Am. Chem. Soc.* **1987**, *109*, 4723. (b) Li, Y.-Z.; Kirby, J. P.; George, M. W.; Popiakoff, M.; Schuster, G. B. *J. Am. Chem. Soc.* **1988**, *110*, 8092.
(13) (a) Borden, W. T.; Gritsan, N. P.; Hadad, C. M.; Karney, W. L.; Kemnitz, C. R.; Platz, M. S. *Acc. Chem. Res.* **2000**, *33*, 765. (b) Karney, W. L.; Borden, W. T. In *Advances in Carbene Chemistry*; Brinker, U. H., Ed.; Elsevier: Amsterdam, 2001; Vol. 3, pp 206−251. (c) Platz, M. S. In *Contemporary Reactive Intermediates*; Moss, R. A., Platz, M. S., Jones, M., Jr., Eds.; Wiley: New York, 2003; in press. (d) Borden, W. T. In *Contemporary Reactive Intermediates*; Moss, R. A., Platz, M. S., Jones, M., Jr., Eds.; Wiley: New York, 2003; in press.

**Scheme 3**
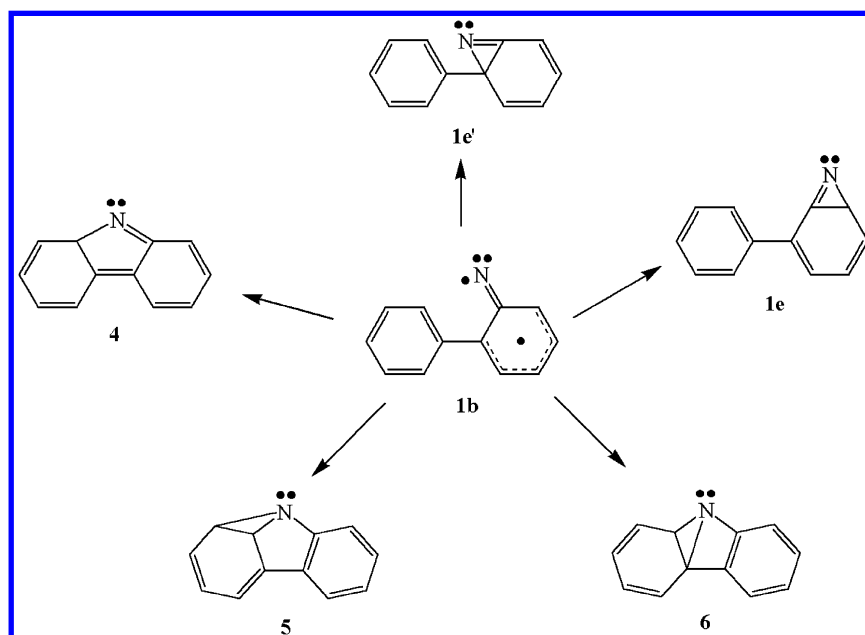


**Computational Methodology.** All calculations were performed with the 6-31G* basis set.[14] Calculations based on density functional theory were carried out with the three-parameter functional of Becke[15] and the correlation functional of Lee, Yang, and Parr (B3LYP).[16] Geometries were optimized and transition structures (TSs) were located at the unrestricted (U)B3LYP level of theory. The geometries of the stationary points and their B3LYP electronic energies are available as Supporting Information.

B3LYP vibrational analyses were performed at each stationary point, to confirm its identity as a minimum or a transition state. The vibrational frequencies were used, without scaling, to convert energy differences into enthalpy differences at 298 K. All of the B3LYP calculations were carried out with the Gaussian 98 suite of programs.[17]

(14/14)CASSCF[18] calculations were performed on singlet *ortho*-biphenylnitrene **1b**, on the three lowest-energy cyclization products (**1e**, **1e′**, **4**, Scheme 3) formed from **1b**, and on the transition structures (TSs) connecting **1b** with each of these three products. For the CASSCF calculations on **1b**, the active space consisted of 14 electrons distributed among the two nonbonding 2p AOs on nitrogen and the six bonding and six antibonding $\pi$ orbitals of the two benzene rings. For the CASSCF calculations on the three cyclization products, the 14 electrons were distributed among the bonding and antibonding orbitals of the six $\pi$ bonds and of the C−N $\sigma$ bond formed in the cyclization reaction.

The (14/14)CASSCF geometries of **1b**, the three lowest-energy cyclization products formed from it, and the three TSs connecting **1b** to these cyclization products are available as Supporting Information. The (14/14)CASSCF/6-31G* calculations were so large that it was impractical to perform vibrational analyses on any of the stationary points that were located with these calculations. Therefore, neither zero-point nor thermal corrections could be made to the CASSCF electronic energies.

To include the effects of dynamic electron correlation,[19] (14/14)CASPT2 calculations[20] were performed at each CASSCF stationary point. The CASSCF and CASPT2 calculations were carried out with the MOLCAS 5.2 suite of ab initio programs.[21] Both the CASSCF and the CASPT2 energies are available as Supporting Information.

**Computational Results and Discussion. Cyclization of 1b.** Possible products of the cyclization of singlet *ortho*-biphenylnitrene (**1b**) are shown in Scheme 3, which also depicts the dominant resonance structure for **1b**.[23b] Phenylnitrenes that are monosubstituted at an ortho position can cyclize at either the substituted or the unsubstituted ortho carbon. In the case of **1b**, these two cyclization modes lead, respectively, to bicyclic azirines **1e** and **1e′**. Nitrene **1b** can also cyclize by attack of nitrogen on an ortho carbon of the phenyl substituent to afford isocarbazole **4**. Finally, if the nitrogen forms $\sigma$ bonds to two

(14) Harihan, P. C.; Pople, J. A. *Theor. Chim. Acta* **1973**, *28*, 213.
(15) Becke, A. D. *J. Chem. Phys.* **1993**, *98*, 5648.
(16) Lee, C.; Yang, W.; Parr, R. G. *Phys. Rev. B* **1998**, *37*, 785.
(17) Frisch, M. J.; Trucks, G. W.; Schlegel, H. B.; Scuseria, G. E.; Robb, M. A.; Cheeseman, J. R.; Zakrzewski, V. G.; Montgomery, J. A., Jr.; Stratmann, R. E.; Burant, J. C.; Dapprich, S.; Millam, J. M.; Daniels, A. D.; Kudin, K. N.; Strain, M. C.; Farkas, O.; Tomasi, J.; Barone, V.; Cossi, M.; Cammi, R.; Mennucci, B.; Pomelli, C.; Adamo, C.; Clifford, S.; Ochterski, J.; Petersson, G. A.; Ayala, P. Y.; Cui, Q.; Morokuma, K.; Malick, D. K.; Rabuck, A. D.; Raghavachari, K.; Foresman, J. B.; Cioslowski, J.; Ortiz, J. V.; Baboul, A. G.; Stefanov, J. V.; Liu, G.; Liashenko, A.; Piskorz, P.; Komaromi, I.; Gomperts, R.; Martin, R. L.; Fox, D. J.; Keith, T.; Al-Laham, M. A.; Peng, C. Y.; Nanayakkara, A.; Gonzalez, C.; Challacombe, M.; Gill, P. M. W.; Johnson, B.; Chen, W.; Wong, M. W.; Andres, J. L.; Gonzalez, C.; Head-Gordon, M.; Replogle, E. S.; Pople, J. A. *Gaussian 98*, revision A.7; Gaussian, Inc.: Pittsburgh, PA, 1998.
(18) Roos, B. O. *Adv. Chem. Phys.* **1987**, *69*, 339.
(19) Borden, W. T.; Davidson, E. R. *Acc. Chem. Res.* **1996**, *29*, 67.
(20) (a) Andersson, K.; Malmqvist, P.-Å.; Roos, B. O.; Sadlej, A. J.; Wolinski, K. *J. Phys. Chem.* **1990**, *94*, 5483. (b) Andersson, K.; Malmqvist, P.-Å.; Roos, B. O. *J. Chem. Phys.* **1992**, *96*, 1218.
(21) Andersson, K.; Barysz, M.; Bernhardsson, A.; Blomberg, M. R. A.; Carissan, Y.; Cooper, D. L.; Cossi, M.; Fleig, T.; Fülscher, M. P.; Gagliardi, L.; de Graaf, C.; Hess, B. A.; Karlström, G.; Lindh, R.; Malmqvist, P.-Å.; Neogrády, P.; Olsen, J.; Roos, B. O.; Schimmelpfennig, B.; Schütz, M.; Seijo, L.; Serrano-Andrés, L.; Siegbahn, P. E. M.; Stålring, J.; Thorsteinsson, T.; Veryazov, V.; Wierzbowska, M.; Widmark, P.-O. *MOLCAS*, version 5.2; Department of Theoretical Chemistry, Chemical Centre: University of Lund, P.O. Box 124, S-221 00 Lund, Sweden, 2001.
(22) The B3LYP/6-31G* energies of **5** and **6**, relative to the UB3LYP energy of **1c**, are given in Table 1. The B3LYP energies of the transition structures connecting **5** and **6** to **1b** are given in the Supporting Information.
(23) (a) Kim, S.-J.; Hamilton, T. P.; Schaefer, H. F. *J. Am. Chem. Soc.* **1992**, *114*, 5349. (b) Hrovat, D. A.; Waali, E. E.; Borden, W. T. *J. Am. Chem. Soc.* **1992**, *114*, 8698. (c) Castell, O.; García, V. M.; Bo, C.; Caballol, R. *J. Comput. Chem.* **1996**, *17*, 42.
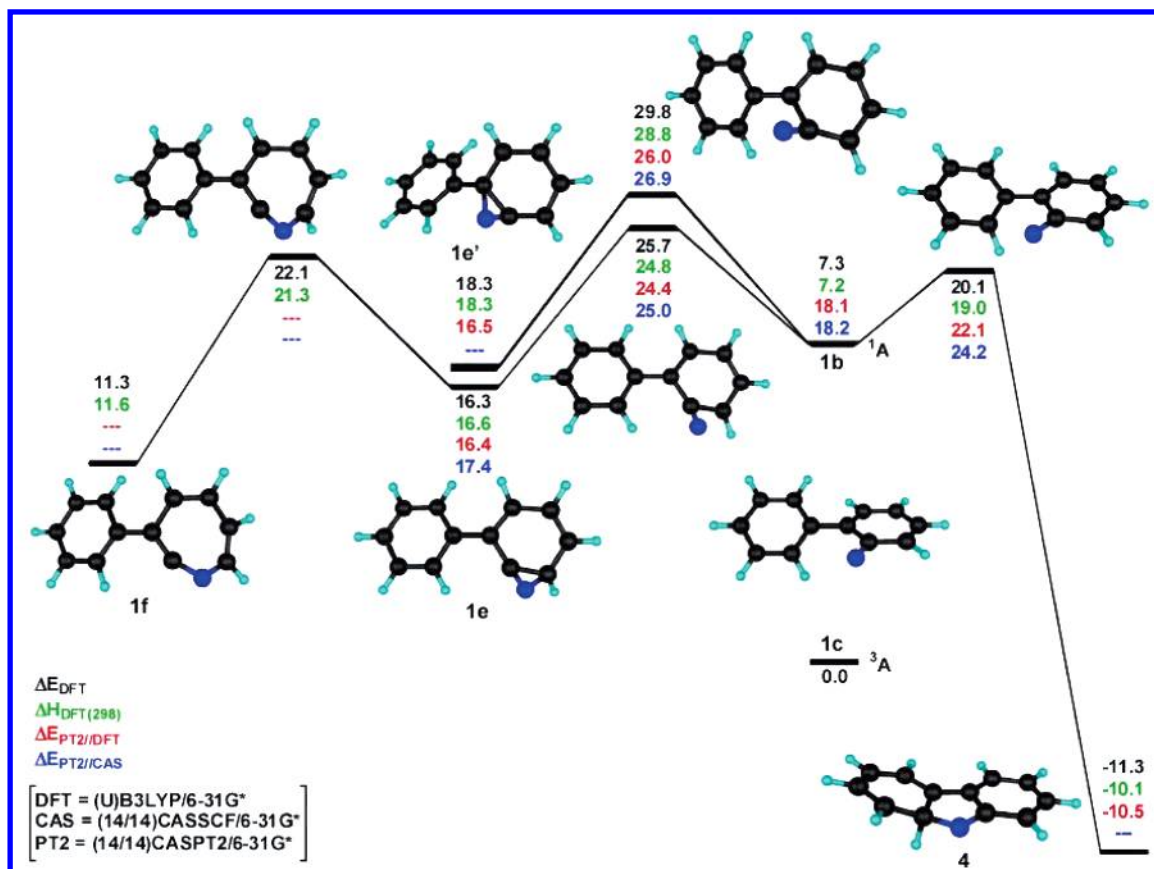
**Figure 1.** (U)B3LYP relative energies and enthalpies and CASPT2 relative energies (kcal/mol) of species involved in the cyclization of singlet *ortho*-biphenylnitrene (**1b**) to azirines (**1e** and **1e′**) and to isocarbazole (**4**), and in the ring opening of **1e** to 3-phenyl-1-azacycloheptatetraene (**1f**).

carbons of the phenyl substituent, tetracyclic aziridines **5** and **6** could also be formed.

B3LYP calculations confirmed the expectation that, of these five possible cyclization products of **1b**, isocarbazole **4** is, by far, the lowest in energy, followed by azirines **1e** and **1e′**. Tetracyclic aziridines **5** and **6** were calculated to be higher still in energy, and the TSs for their formation were also computed to be considerably higher in energy than the TSs for formation of **1e**, **1e′**, and **4**.[22] Therefore, (14/14)CASSCF and CASPT2 calculations were performed only on **1e**, **1e′**, and **4** and on the TS connecting each of them to **1b**.

The energies obtained by our (U)B3LYP and CASPT2 calculations on **1e**, **1e′**, **4**, and the three TSs are summarized in Figure 1. The energies are given relative to that of the triplet ground state **1c**. With the exception of the lowest singlet state **1b**, the (U)B3LYP and CASPT2 energies are in fair agreement, with the largest difference being less than 4 kcal/mol.

The UB3LYP calculations give a singlet−triplet energy difference between **1b** and **1c** that is smaller by >10 kcal/mol than the CASPT2 value. Not surprisingly, the CASPT2 value is similar to the values found both computationally[23] and experimentally[24] for phenylnitrene (**2b**). The UB3LYP value for the singlet−triplet splitting between **1b** and **1c** appears to be in error.

The reason for this error is that the lowest singlet states of phenylnitrenes have the same orbital occupancies as the lowest

triplets.[23] In both states, one electron occupies the nonbonding 2p AO on nitrogen that lies in the plane of the benzene ring, and the other nonbonding electron is delocalized into the $\pi$ system of the benzene ring. However, a UB3LYP "singlet" wave function, for instance, with an $\alpha$-spin electron in the nonbonding 2p AO that is localized on nitrogen and a $\beta$-spin electron in the nonbonding $\pi$ orbital, is actually a mixture of pure singlet and triplet wave functions.[25] Therefore, such a wave function provides a very poor description of the actual singlet state.

The fact that the "singlet" UB3LYP wave function for **1b** is really a mixture of singlet and triplet states is evident in the value of $S^2 = 1.03$ for this wave function. The UB3LYP wave function for the triplet state of **1** has $S^2 = 2.05$, and a pure singlet wave function would have $S^2 = 0$. Therefore, the UB3LYP "singlet" wave function for **1b** is approximately a 1:1 mixture of pure singlet and triplet wave functions.

Because the UB3LYP "singlet" wave function for **1b** is about one-half comprised of the wave function for the triplet, the UB3LYP value for the energy difference between this "singlet" state and the triplet is smaller by 11 kcal/mol than the CASPT2 value for the singlet−triplet splitting. However, this UB3LYP error is not limited to just the singlet−triplet splitting in **1b**; the same type of error is present in all of the energy differences between the UB3LYP "singlet" nitrene and the other stationary points shown in Figure 1. Therefore, the UB3LYP values for $\Delta H^{\ddagger}$ for cyclization of **1b** are much less reliable than the

(24) (a) Travers, M. J.; Cowles, D. C.; Clifford, E. P.; Ellison, G. B. *J. Am. Chem. Soc.* **1992**, *114*, 8699. (b) McDonald, R. N.; Davidson, S. J. *J. Am. Chem. Soc.* **1993**, *115*, 10857.

(25) See, for example: Bally, T.; Borden, W. T. In *Reviews in Computational Chemistry*; Lipkowitz, K. B., Boyd, D. B., Eds.; Wiley-VCH Publishers: New York, 1999; Vol. 13, pp 1−97.

differences between the CASPT2 energies of each of the TSs and the CASPT2 energy of pure ($S^2 = 0$) singlet **1b**.

Both B3LYP and CASPT2 find the energy differences between the TSs leading from **1b** to benzazirines **1e** and **1e′** to be larger than the energy differences between the benzazirines themselves. As has been discussed elsewhere,[26] steric effects, due to an ortho substituent, are larger in the TS for phenylnitrene cyclization at the substituted carbon than those in the 3-substituted bicyclic azirine formed by this reaction.

As shown in Figure 1, the CASPT2/6-31G*//CASSCF/6-31G* energy difference between **1b** and the TS for its cyclization to **1e** is 6.8 kcal/mol. Calculations at the same level of theory predict an energy difference of 8.5 kcal/mol between singlet phenylnitrene **2b** and the TS for its cyclization to **2e**.[27]

The latter energy difference is known to be too high by 2−3 kcal/mol,[27] and the error in the energy difference between **1b** and the TS for its cyclization to **1e** is likely to be about the same size. If one assumes that the vibrational energy corrections to both energy differences are the same, CASPT2 predicts that **1b** should cyclize to **1e** with an enthalpy of activation that is ca. 2 kcal/mol lower than that for cyclization of the parent singlet phenylnitrene **2b**.

It is entirely possible that the phenyl substituent in **1b** provides some electronic stabilization for the TS leading to **1e′** (Scheme 3), but there is no reason to believe that this is the case in the TS leading to **1e**.[28] Instead, the phenyl group probably lowers the enthalpy of activation for cyclization by destabilizing **1b** sterically. The ortho hydrogen on the phenyl substituent that is closest to the nitrogen is separated from the nitrogen by only 2.60 Å in the CASSCF geometry of **1b**, and the proximity of these two atoms results in the nitrogen being bent out of the plane of the aromatic ring, albeit by just 4.0°.

Although the more stable of the two bicyclic azirines (**1e**) is >27 kcal/mol higher in energy than isocarbazole **4**, the UB3LYP and CASPT2 energies of the TSs leading to **1e** and **4** are much more nearly the same. Both TSs apparently occur early enough along the reaction coordinate that the large energy difference between **1e** and **4** is barely manifested in the relative energies of the TSs leading to these two cyclization products.

Nevertheless, as shown in Figure 1, at both the UB3LYP and the CASPT2 levels of theory, the TS leading to the more stable product (**4**) is lower in energy than the TS leading to the less stable product (**1e**). The difference between the UB3LYP energies of the two TSs (5.6 kcal/mol) is nearly the same as the difference between their enthalpies (5.8 kcal/mol). Thus, UB3LYP predicts that **1b** should cyclize exclusively to **4** and that little, if any, **1e** should be formed. However, this prediction appears to be inconsistent with the experimental results of Sundberg and co-workers,[3a,b] which suggest that $k_c$ is comparable to $k_{car}$ in size (Scheme 1).

In contrast, the CASPT2//CASSCF calculations predict that the TS leading to **4** is lower in energy than the TS leading to **1e** by less than 1 kcal/mol. Therefore, unlike UB3LYP, the CASPT2 TS energies predict that both **1e** and **4** should be formed from **1b**.

On the basis of the UB3LYP results in Figure 1, it seems likely that the difference between the CASPT2 enthalpies of

the TSs leading to **1e** and **4** is almost exactly the same as the difference between their CASPT2 energies. Thus, like the CASPT2 energies, the enthalpies of the TSs leading to **1e** and **4** might be expected to differ by only ca. 1 kcal/mol.

If this is, in fact, the case, at 298 K, entropy should make **1e**, not **4**, the kinetically favored product. In the cyclization of **1b** to **4**, as the five-membered ring is formed, internal rotation about the bond between the two phenyl rings in **1b** must be frozen out. In contrast, in forming **1e** from **1b**, this low-frequency mode should be little affected. Consequently, the entropy of the TS leading to **1e** should be ca. 5 cal mol$^{-1}$ K$^{-1}$ higher than that of the TS leading to **4**.[29]

In fact, UB3LYP vibrational analyses find that, at 298 K, the TS leading to **1e** does have a higher entropy than the TS leading to **4** by 5.7 cal mol$^{-1}$ K$^{-1}$. At this temperature, the higher entropy of the TS leading to **1e** would contribute 1.7 kcal/mol to making its free energy lower than that of the TS leading to **4**. Therefore, combining the CASPT2 energies with the results of UB3LYP vibrational analyses, **1e**, rather than the much lower energy **4**, should be the kinetically favored product around room temperature.

Why does UB3LYP predict that the TS leading to **4** is significantly lower in energy (and enthalpy) than the TS leading to **1e**? The origin of this apparently spurious result is easily found by comparing the $S^2$ values for the "singlet" wave functions at the two UB3LYP TSs. The value of $S^2 = 0.58$ for the UB3LYP wave function for the TS leading to **4** is considerably higher than the value of $S^2 = 0.21$ for the UB3LYP wave function for the TS leading to **1e**.

The reason for this difference in $S^2$ values between the two TSs is that, not surprisingly, the more exothermic reaction has the earlier TS. For example, in the TS leading to **4**, the B3LYP length of the forming C−N bond (2.11 Å) is 0.13 Å greater than that in the TS leading to **1e**. This difference is 0.06 Å larger still in the CASSCF than in the UB3LYP TSs for cyclization of **1b**.

The greater length of the forming C−N bond in the TS leading to **4** means that the UB3LYP energy difference between the "singlet" and the triplet, which lies above it, is only 3.3 kcal/mol in this TS, as compared to 14.2 kcal/mol in the TS leading to **1e**. Therefore, contamination of the "singlet" UB3LYP wave function, by the presence of the triplet wave function, is less energetically costly in the TS leading to **4** than in the TS leading to **1e**. This is why $S^2$ is considerably larger for the former UB3LYP wave function than for the latter.

The greater admixture of triplet character into the "singlet" UB3LYP wave function for the TS leading to **4** artificially lowers its energy relative to that of the TS leading to **1e**. Thus, the large difference between $S^2$ values of the UB3LYP "singlet" wave functions for the TSs leading to **4** and **1e** is indicative of the reason the former TS is spuriously found by UB3LYP to be 5.8 kcal/mol lower than the TS leading to **1e**.

The potential hazards of performing unrestricted calculations on singlet diradicals with large singlet−triplet energy separations are well known.[25] Less appreciated is the fact that spin contamination can cause unrestricted calculations to give spurious results for molecules and TSs that are not truly singlet diradicals but which do have $S^2 \neq 0$. As shown by the results

(26) Karney, W. L.; Borden, W. T. *J. Am. Chem. Soc.* **1997**, *119*, 3347.
(27) Karney, W. L.; Borden, W. T. *J. Am. Chem. Soc.* **1997**, *119*, 1378.
(28) Gritsan, N. P.; Likhotvorik, I.; Tsao, M.-L.; Çelebi, N.; Platz, M. S.; Karney, W. L.; Kemnitz, C. R.; Borden, W. T. *J. Am. Chem. Soc.* **2001**, *123*, 1425.

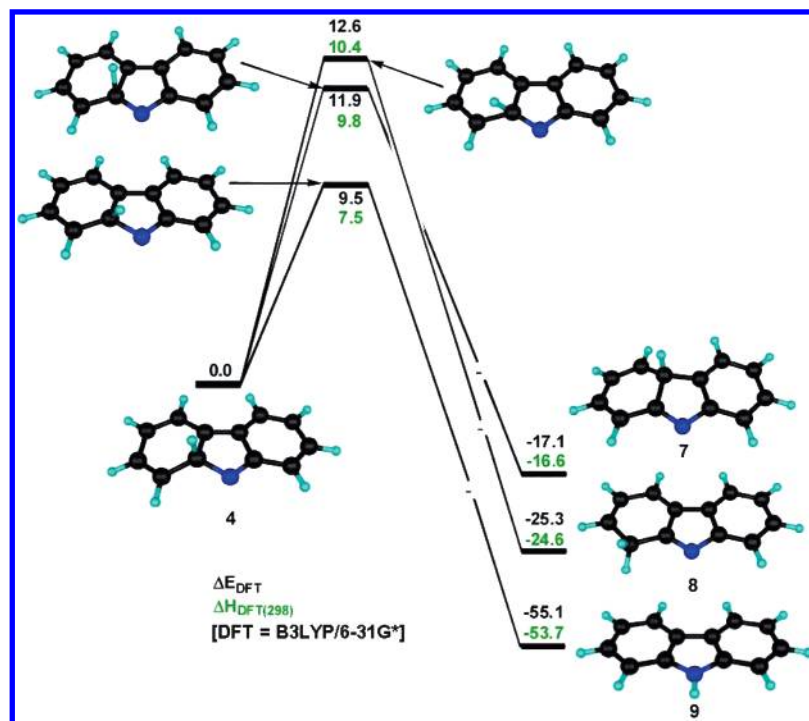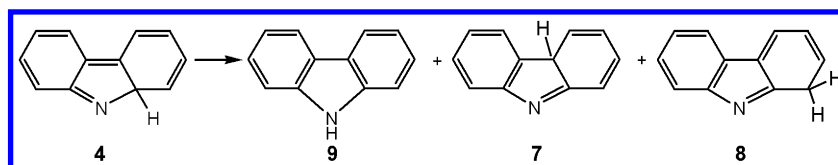(29) Benson, S. W. *Thermochemical Kinetics*, 2nd ed.; Wiley: New York, 1976; pp 65−67.

**Figure 2.** B3LYP/6-31G* relative energies and enthalpies (kcal/mol) of species involved in the 1,5-hydrogen shifts of isocarbazole (**4**) to form three different isomers of **4** (**7**, **8**, and **9**).

**Scheme 4**



for the TSs leading to **1e** and **4**, if two stationary points have rather different values of $S^2$, comparing their relative UB3LYP energies can lead to predictions that are both quantitatively and qualitatively incorrect.

**Ring Opening of 1e.** UB3LYP calculations on the cyclization of "singlet" **1b** to **1e** and **4** are made unreliable by the spin contamination in the wave functions for not only the nitrene, but also for the TSs leading to **1e** and **4**. However, both **1e** and **4** are closed-shell molecules. Therefore, there is no reason to expect B3LYP calculations to be inadequate for describing the PESs for the reactions of **1e** and **4**, after their formation from **1b**. Consequently, given the high computational cost of (14/14)CASSCF geometry optimizations and (14/14)CASPT2 single-point calculations, we performed only B3LYP calculations on the ring opening of **1e** to 1-aza-3-phenyl-1,2,4,6-cycloheptatetraene (**1f**) and on the three possible 1,5-hydrogen shifts that can occur in **4**.

As shown in Figure 1, the B3LYP barrier height for ring opening of **1e** to **1f** is computed to be $\Delta H^{\ddagger} = 4.7$ kcal/mol. This barrier height is 1.1 kcal/mol higher than the B3LYP barrier height for ring opening of the unsubstituted 7-azabicyclo[4.1.0]-heptatriene **2e**. The latter azirine intermediate has not been detected in the ring expansion of phenylnitrene.[13,27] However, the 30% higher barrier computed for ring opening of **1e** to **1f** might make it possible to observe **1e** in the ring expansion of **1b**.

The B3LYP enthalpy of activation for rearrangement of azacycloheptatetraene **1f** back to singlet nitrene **1b** is computed

to be only 13.2 kcal/mol, with the rate-determining step being passage over the TS connecting **1e** to **1b**. Because the CASPT2 energy difference between **1e** and the TS connecting it to **1b** is 1.8 kcal/mol smaller than the B3LYP energy difference, 11.4 kcal/mol is probably a more accurate value for the expected barrier height for rearrangement of **1f** back to **1b**. Thus, **1f** is predicted to provide a source for regenerating the singlet nitrene, after the initial cyclization of **1b** to a mixture of **1e** and **4**, and the height of the calculated barrier that separates **1f** from **1b** is in excellent agreement with the value of 11.5 kcal/mol inferred from the experiments of Lehman and Berry.[5]

Isocarbazole **4** is computed to be more than 20 kcal/mol lower in enthalpy than **1f**. Therefore, unless chemically trapped, all of the **1f** that is initially formed from **1b** should ultimately isomerize to **4** by a pathway involving ring closure of **1f** to **1e**, ring opening of **1e** to **1b**, and, finally, passage of **1b** over the TS leading to ring closure to **4**.

**1,5-Hydrogen Shifts in Isocarbazole 4.** After formation of **4**, either by direct cyclization of **1b** or by isomerization of **1f** back to **1b**, isocarbazole **4** can undergo 1,5-hydrogen shifts to afford three different isomers of **4**. These are depicted in Scheme 4.

The B3LYP energies and enthalpies of **7**−**9**, relative to those of **4**, are given in Figure 2. Also shown is the B3LYP energy and enthalpy of the TS that connects each of the rearrangement products of isocarbazole **4** .

Not surprisingly, the lowest energy of the isomers shown in Figure 2 is predicted to be carbazole **9**, followed by azaben-

**Table 1.** Energies (ΔE, kcal/mol), Relative to **1c**, of Intermediates Calculated Using the (14,14)CASPT2//CASSCF(14,14)/6-31G* Method for Singlet (**1b**) and Triplet (**1c**) *ortho*-Biphenylnitrenes and by the (U)B3LYP/6-31G* Method for **1e**, **1f**, and **4**–**9**;[a] Absorption Maxima (λ, nm) and Oscillator Strengths (*f*), Computed Using Time-Dependent DFT Calculation at the (U)B3LYP/6-31G* Level of Theory, Are Also Shown

| compound | ΔE | λ, nm (*f*) | λ, nm (*f*) | λ, nm (*f*) | λ, nm (*f*) | λ, nm (*f*) |
|---|---|---|---|---|---|---|
| **1b** | 18.2 | | | | | |
| **1c** | 0.0 | 479 (0.027) | 357 (0.013) | 342 (0.076) | 335 (0.012) | 305 (0.063) |
| **1e** | 16.6 | 343 (0.174) | 300 (0.210) | | | |
| **1f** | 11.6 | 400 (0.001) | 378 (0.019) | | | |
| **4** | −10.1 | 474 (0.145) | 362 (0.020) | 306 (0.119) | | |
| **5** | 37.9 | 462 (0.007) | 322 (0.031) | 275 (0.097) | | |
| **6** | 27.3 | 322 (0.029) | 280 (0.018) | | | |
| **7** | −26.7 | 367 (0.164) | 315 (0.012) | 297 (0.010) | | |
| **8** | −34.8 | 427 (0.014) | 361 (0.289) | 281 (0.055) | | |
| **9** | −63.8 | 299 (0.029) | 271 (0.117) | | | |

[a] Differences in ZPE are included in all of the DFT results.

zofulvene **8**, which is calculated to be lower in energy than **7**. Compounds **7**–**9** are all predicted to be lower in energy than **4**, because they each contain at least one benzene ring, whereas neither six-membered ring in **4** is aromatic.

Figure 2 shows that the B3LYP enthalpies of the TSs leading from **4** to **7**–**9** differ by much less than the enthalpies of **7**–**9**. Therefore, although **9** is predicted to be the isomer, favored both kinetically and thermodynamically, it is possible that small amounts of **7** and **8** might also be formed from **4**.

Isomerization back to **4** provides the lowest-energy pathway from **7** and **8** to **9**, but the barriers separating **7** and **8** from **4** are calculated to be in the range of 25−35 kcal/mol. Therefore, if small amounts of **7** and **8** were initially formed from **4**, they should be kinetically stable enough to be detectable, before they isomerize to **9**.

Although **4**, when formed from cyclization of **1b**, should contain more than 30 kcal/mol of excess energy, in solution this excess energy is likely to be quenched by collisions with solvent molecules before **4** can undergo 1,5-hydrogen shifts to form **7**–**9**. The barrier to rearrangement of **4** to **9** is predicted by B3LYP to be ΔH‡ = 7.5 kcal/mol. This barrier is high enough that laser flash photolysis studies should, at least in principle, allow detection of isocarbazole **4** as an intermediate in the formation of carbazole **9**.

**Calculated UV−Vis Spectra.** To assist in the experimental identification of the reactive intermediates in Scheme 1, the electronic spectra of **1c**, **1e**, and **1f**, of isocarbazole **4**, and of tetracyclic aziridines **5** and **6** were calculated, using time-dependent (TD)DFT theory with the random phase approximation.[30] The results are presented in Table 1.

As shown in Table 1, **4** is predicted to have an intense absorption band in the visible region (474 nm). Although calculations predict that **5** has an absorption band with a maximum at 462 nm, it is predicted to be much weaker than that in **4**. Intermediate
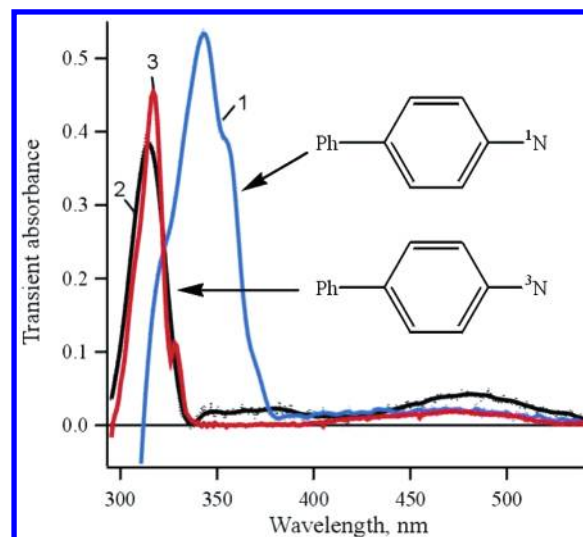
(30) Casida, M. E.; Jamorski, C.; Casida, K. C.; Salahub, D. R. *J. Chem. Phys.* **1998**, *108*, 4439.



**Figure 3.** Transient UV absorption spectra observed in a window of 30 ns, following LFP of *para*-biphenyl azide (**3a**) in pentane at 198 K. Spectrum 1 was recorded just after the laser pulse and is assigned to singlet *para*-biphenylnitrene (**3b**). Spectrum 2 was obtained 250 ns after the laser pulse and is assigned to triplet *para*-biphenylnitrene (**3c**). Spectrum 3 is the persistent UV spectrum of **3c**, produced by photolysis (10 s, 254 nm) of **3a** in a methylcyclohexane glass at 77 K.

**6**, which is less conjugated than **5**, has no predicted absorption in the visible region. Polyenes **7** and **8** are both predicted to have an intense absorption band around 360 nm. The experimental UV spectrum of carbazole **9**, with λmax = 292 nm and ε = 1.58 × 10⁴ M⁻¹ cm⁻¹ (95% ethanol, 5% water), is reproduced satisfactorily by the TD-DFT calculations.

**II.2. Experimental Studies. LFP of *para*-Biphenyl Azide 3a.** To investigate the effect of a phenyl substituent on the rate constants for intersystem crossing and cyclization of a singlet arylnitrene to an azirine, we first performed a laser flash photolysis (LFP) study of *para*-biphenyl azide. LFP at 266 nm (50 mJ, 5 ns) of *para*-biphenyl azide (**3a**, Scheme 2) in pentane at 198 K produces transient UV spectrum 1 in Figure 3. This spectrum (λmax = 343 nm) is attributed to singlet *para*-biphenylnitrene (**3b**), due to the similarity of spectrum 1 to the transient UV spectrum (λmax = 335 and 352 nm) of the parent singlet phenylnitrene (**2b**).[7,9] The decay of transient spectrum 1 is accompanied by an increase in the intensity of spectrum 2, which we attribute to triplet nitrene **3c**. Indeed, transient spectrum 2, obtained in pentane solution at 198 K, is very similar to the persistent UV spectrum of triplet nitrene **3c** in a methylcyclohexane glass at 77 K (spectrum 3 in Figure 3).

The lifetime of the parent singlet phenylnitrene (**2b**) is ∼1 ns in pentane at ambient temperature.[7,9] The lifetime of **3b** at ambient temperature, 13 ns in pentane and 9 ns in acetonitrile, is significantly longer than that of **2b**.

Transient spectrum 1 in Figure 4 was recorded at 323 K in hexane over a window of 30 ns following LFP of azide **3a**. The spectrum reveals the presence of azacycloheptatetraene **3f** (broad absorption band with maximum at ∼350 nm), as well as a small amount of triplet nitrene **3c**. Both species can also be seen in spectrum 2 in Figure 4, recorded at 296 K in pentane at 200 ns after the laser pulse. The UV spectra of **3f** and **3c** greatly resemble those of the parent azacycloheptatetraene (**2f**) and the parent triplet phenylnitrene (**2c**), respectively.[7,9] A *para*-
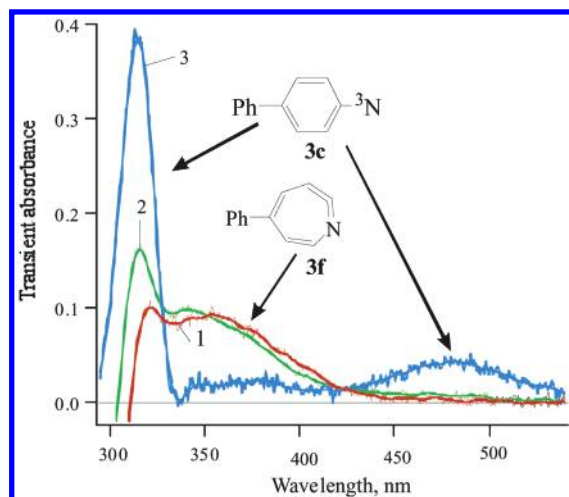
**Figure 4.** Transient UV absorption spectra observed in a window of 30 ns, following LFP of *para*-biphenyl azide (**3a**). Spectrum 1 was obtained at 323 K in hexane just after the laser pulse. Spectrum 2 was recorded at 296 K in pentane 200 ns after the laser pulse. Spectrum 3, obtained at 198 K in pentane 250 ns after the laser pulse, is the same as spectrum 2 in Figure 3 and is assigned to triplet *para*-biphenylnitrene (**3c**). At 198 K, **3c** is the dominant product formed from **3b** (see text).
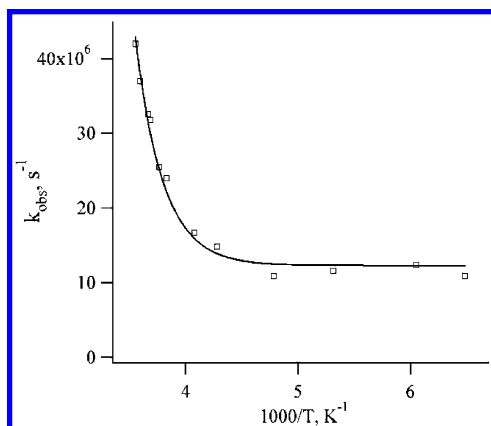


**Figure 5.** Temperature dependence of the observed rate constant ($k_{obs}$) for the decay of singlet *para*-biphenylnitrene (**3b**) in pentane.

phenyl group apparently has little influence on the UV spectra of **2f** and **2c**.

The decay of the transient absorption of singlet nitrene **3b** in pentane can be fit to an exponential function, which yields an observed rate constant ($k_{obs}$). The magnitude of $k_{obs}$ decreases as the temperature decreases until a limiting value of $k_{obs}$ is reached (Figure 5). The same type of temperature dependence has been found in $k_{obs}$ for the disappearance of singlet phenylnitrene (**2b**)[9] and a series of its derivatives.[13,28,31–33] The temperature-independent rate constants for decay of the singlet nitrenes, observed at low temperatures, are the rate constants for intersystem crossing of the singlet nitrenes to the lowest triplet states ($k_{isc}$).

*para*-Biphenyl azide **3a**, immobilized in glassy 3-methylpentane at 77 K, was also studied by LFP. Singlet nitrene **3b** was observed immediately after the 266 nm laser pulse (Figure 1 in the Supporting Information). At 77 K, the observed rate constant
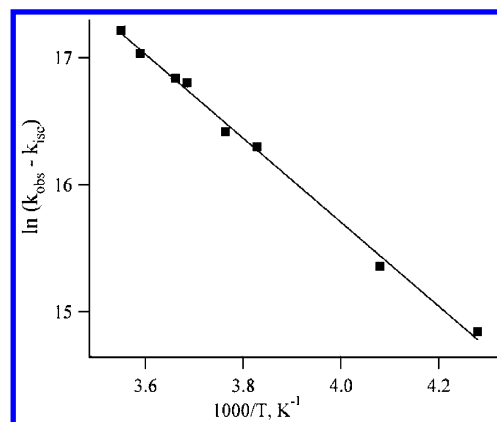
(31) Gritsan, N. P.; Platz, M. S. *Adv. Phys. Org. Chem.* **2001**, *36*, 255.
(32) Gritsan, N. P.; Gudmundsdóttir, A. D.; Tigelaar, D.; Platz, M. S. *J. Phys. Chem. A* **1999**, *103*, 3458.
(33) Gritsan, N. P.; Gudmundsdóttir, A. D.; Tigelaar, D.; Zhu, Z.; Karney, W. L.; Hadad, C. M.; Platz, M. S. *J. Am. Chem. Soc.* **2001**, *123*, 1951.

**Figure 6.** Arrhenius treatment of the cyclization rate constant ($k_c = k_{obs} - k_{isc}$) for singlet *para*-biphenylnitrene (**3b**) in pentane.

for decay of **3b** was $k_{obs} = (9.3 \pm 0.1) \times 10^6$ s$^{-1}$ ($\tau = 108 \pm 1$ ns). The decay of **3b** at 77 K was accompanied by the growth ($k_{obs} = (9.3 \pm 0.4) \times 10^6$ s$^{-1}$) of the absorption of triplet nitrene **3c** with a maximum at 320 nm. This value of $k_{obs}$ ($\equiv k_{isc}$) is in good agreement with the value of $k_{isc} = (12 \pm 1) \times 10^6$ s$^{-1}$ obtained by extrapolation of the solution phase data. Therefore, it is clear that $k_{isc}$ does not vary with temperature.

The temperature independence of $k_{isc}$ allows $k_c$ at any temperature to be deduced from eq 1. The validity of this equation has been previously assumed in studies of the parent singlet phenylnitrene (**2b**)[12] and of substituted singlet phenylnitrenes,[13,28,31–33]

$$k_{obs} = k_c + k_{isc} \tag{1}$$

The elementary rate constants for cyclization ($k_c$) and intersystem crossing ($k_{isc}$) are defined in Scheme 2.

Arrhenius treatment of $k_c$ is presented in Figure 6. The Arrhenius parameters for cyclization of singlet nitrene **3b**, along with the data for parent singlet phenylnitrene (**2b**), show that the *para*-phenyl group in **3b** increases $k_{isc}$ by a factor of 4, but retards the rate of cyclization by raising the barrier to this reaction by 1.2 kcal/mol.

Calculations reveal that singlet phenylnitrene (**2b**) and its derivatives have open-shell electronic structures.[13,23,34] As depicted in eq 2, the cyclization of a singlet arylnitrene is essentially the collapse of an iminylcyclohexadienyl diradical.[13,26,27]
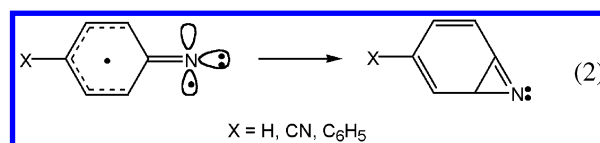


A radical-stabilizing phenyl substituent in the para position reduces the spin density at the ortho position, thereby decelerating cyclization of **3b** (X = Ph), relative to that of **2b** (X = H). The same effect has previously been observed for X = CN.[28]

**LFP of *ortho*-Biphenyl azide 1a.** As was described in Section II.1, our calculations predict that LFP studies should allow detection of azacycloheptatetraene **1f** and isocarbazole **4** as reactive intermediates in the formation of carbazole **9** from

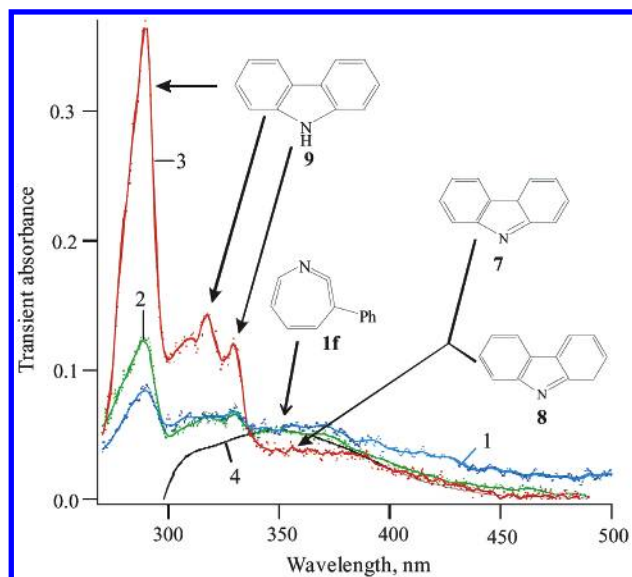(34) Johnson, W. T. J.; Sullivan, M. B.; Cramer, C. J. *Int. J. Quantum Chem.* **2001**, *85*, 492.

**Figure 7.** Transient absorption spectra detected over a window of 20 ns following LFP of *ortho*-biphenyl azide **1a** in pentane at ambient temperature. Spectra were obtained at (1) 55 ns, (2) 1 $\mu$s, and (3) 5 ms after the laser pulse. Line (4) is the spectrum of 5-methyl-1-azacycloheptatetraene, formed by LFP of *para*-methylphenyl azide.

singlet *ortho*-biphenylnitrene (**1b**). In addition, the calculations hold out the possibility that it might also be possible to detect bicyclic azirine **1e** as an intermediate in the formation of **1f** from **1b** and to observe one or both of the higher energy isomers of **9** (i.e., **7** and **8**), formed by alternative 1,5-hydrogen shifts in **4**. Guided by these predictions, we performed experiments on *ortho*-biphenyl azide (**1a**), using a combination of laser flash photolysis (LFP), with UV detection and nanosecond time resolution, and time-resolved infrared (TRIR) spectroscopy.

Figure 7 shows the transient UV spectra recorded at three different time intervals following the LFP of **1a**. Spectrum 3, recorded 5 ms after the laser pulse, is essentially the same as the UV spectrum of carbazole **9**. Thus, the spectra in Figure 7 demonstrate that, in agreement with previous flash photolysis data,[3c,5] **9** is mainly formed on the millisecond time scale in pentane. The time constant for formation of **9** actually is about 1 ms at ambient temperature.

The formation of **9** is accompanied by the concurrent decay of a broad transient absorption between 330 and 380 nm, seen

in spectra 1 and 2 in Figure 7. The similarity of this absorption to that seen in spectra 1 and 2 in Figure 4 and to the spectrum of 5-methyl-1-azacycloheptatetraene (spectrum 4 in Figure 7) leads us to attribute this broad absorption to formation of 3-phenyl-1-azacycloheptatetraene (**1f**).

The intensity of the transient absorption at $\lambda > 350$ nm, seen milliseconds after the laser pulse in spectrum 3 of Figure 7, is much greater than that which can be ascribed to carbazole **9**. This is in accord with Sundberg and co-workers' previous observations of transient intermediates whose decay is slower than the initial rate of formation of **9**. As discussed in Section III, we believe that this absorption at $\lambda > 350$ nm is due to isocarbazoles **7** and **8**.

The formation of carbazole **9** in solution is at least biphasic. In addition to the formation of **9** on the millisecond time scale, discovered previously,[3] spectrum 1 in Figure 7 shows some formation of **9** on the nanosecond time scale as well. As shown in Figure 8A, the nanosecond growth of carbazole absorption at 290 nm was accompanied by the nanosecond decay of a transient absorption in the visible region between 400 and 500 nm. The growth of the absorption at 290 nm and the decay of the broad absorption at longer wavelengths can each be fit with an exponential function. The time constants for the growth and decay functions are the same within experimental error and equal to $70 \pm 5$ ns in pentane at ambient temperature.

At ambient temperatures, the transient absorption in the visible region was very broad and not particularly intense. Therefore, it was difficult to define the band maximum. However, at 161 K, a more intense absorption in the visible region was seen with an apparent maximum at ~430 nm. As shown in Figure 9, at 161 K, decay of this band was again accompanied by the growth of carbazole absorption at 290 nm.

Figure 10 depicts the transient spectra detected after LFP of **1a** at ambient temperature in acetonitrile. Most of the carbazole **9** produced in acetonitrile was formed hundreds of microseconds after the laser pulse, just as was observed previously in pentane. Carbazole growth was accompanied by the decay of a transient absorption band with a maximum near 350 nm. This band was more pronounced in acetonitrile (Figure 10) than in pentane (Figure 7). More significantly, unlike the spectra obtained when **1a** was subjected to LFP in pentane, transient absorption in the visible region (400−500 nm) was not seen in the spectra
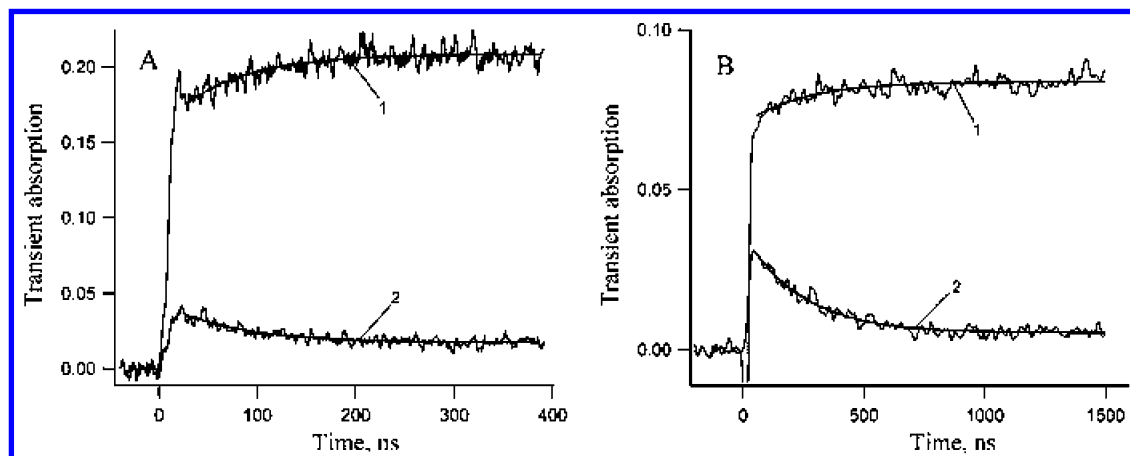


**Figure 8.** Changes in the transient absorption at (1) 290 nm and (2) 460 nm, detected after LFP of (A) *ortho*-biphenyl azide (**1a**) and (B) its perdeutero-substituted derivative (**1a**-$d_9$) in pentane at ambient temperature.
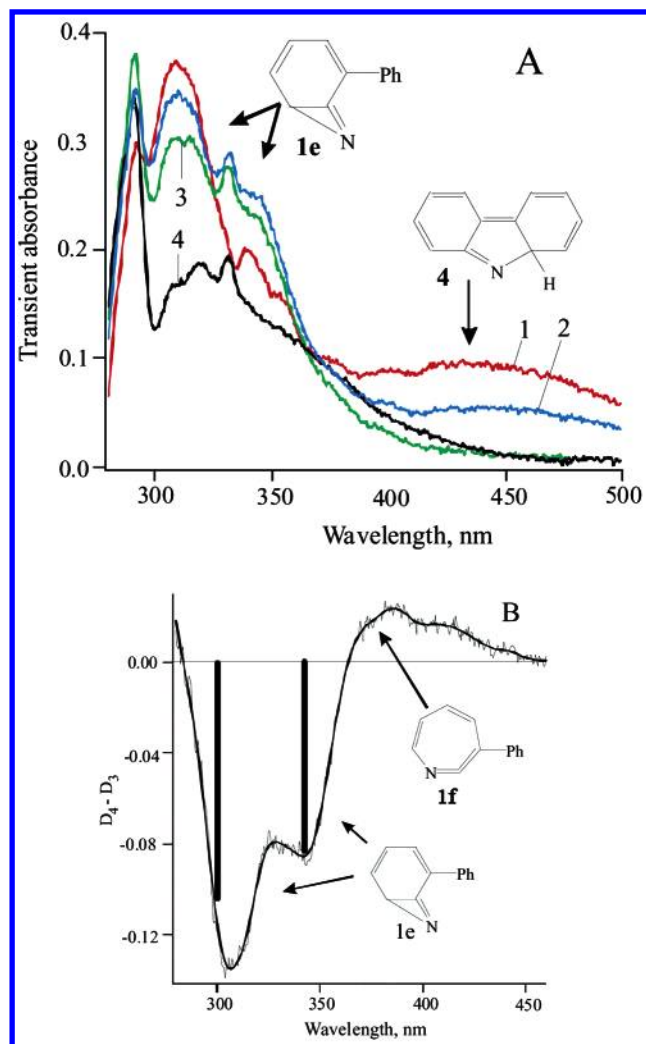
**Figure 9.** (A) Transient absorption spectra detected over a window of 30 ns, following LFP of *ortho*-biphenyl azide **1a** in pentane at 161 K. The spectra shown were obtained: (1) 30 ns, (2) 1 μs, (3) 4 μs, and (4) 150 μs after the laser pulse. Spectrum 1 is contaminated in the region of 320−380 nm by the negative contribution of fluorescence of carbazole, which is formed during the laser pulse (∼5 ns). (B) The difference spectrum obtained by subtracting the transient spectrum obtained 4 μs after the laser pulse (3) from that obtained 150 μs after the laser pulse (4). The computed positions and relative oscillator strengths of the absorption bands of benzazirine **1e** are depicted as solid vertical lines.

obtained in acetonitrile. In the latter solvent, some carbazole was formed faster than the time resolution of the spectrometer (∼5 ns).

**TRIR Spectroscopy.** The photochemistry of *ortho*-biphenyl azide (**1a**) was also studied by TRIR spectroscopy. The characteristic IR absorptions of azacycloheptatetraenes[9,35] around 1870 cm$^{-1}$ make TRIR an ideal technique for investigating whether **1f** serves as a reservoir for singlet nitrene **1b**, which subsequently cyclizes to isocarbazole **4** and ultimately forms **9**.

Figure 11A depicts the IR spectra of azide **1a** (negative peaks) and carbazole (positive peaks) in acetonitrile-$d_3$. The most intense line in the vibrational spectrum of **9** has its maximum at 1241 cm$^{-1}$. Following LFP excitation (YAG laser, 266 nm) of **1a** in acetonitrile, this band of **9** grew (Figure 11B). The characteristic ketenimine IR band of azacycloheptatetraene (**1f**) at 1868 cm$^{-1}$ was also detected (Figure 11C).

(35) (a) Chapman, O. L.; Le Roux, J.-P. *J. Am. Chem. Soc.* **1978**, *100*, 285. (b) Hayes, J. S.; Sheridan, R. S. *J. Am. Chem. Soc.* **1990**, *112*, 5879.
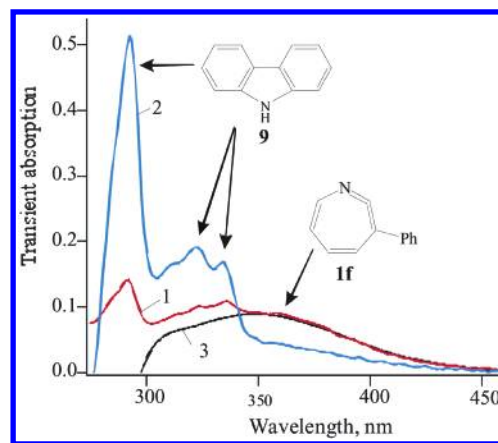
**Figure 10.** Transient absorption spectra detected over a window of 20 ns, following LFP of *ortho*-biphenyl azide **1a** in acetonitrile at ambient temperature. The spectra shown were obtained: (1) 50 ns and (2) 1.5 ms after the laser pulse. Curve 3 is the spectrum of 5-methyl-1-azacycloheptatetraene, formed by LFP of *para*-methylphenyl azide.

The 1868 cm$^{-1}$ band appears faster than the time resolution of the apparatus (about 100 ns) and decays on the microsecond time scale (Figure 12). The decay was fit to an exponential function, giving a rate constant of $k_{az} = (8.3 \pm 0.8) \times 10^3$ s$^{-1}$.

The kinetics of carbazole growth on this time scale were monitored at 1241 cm$^{-1}$ and are also shown in Figure 12. The carbazole growth kinetics, as followed by TRIR spectroscopy, were fit to an exponential function and yielded a rate constant of $(11 \pm 1) \times 10^3$ s$^{-1}$. The rate constant ($k_{az}$) for decay of **1f** is probably equal, within experimental error, to the rate constant for formation of **9**, and both rate constants are close to the value measured by Sundberg et al. ($k = 9.8 \times 10^3$ s$^{-1}$)[3c] for the appearance of **9** in acetonitrile. The TRIR experiments thus demonstrate that azacycloheptatetraene **1f** does indeed serve as a source of **9** on the 100 μs time scale, in acetonitrile, presumably via the mechanism shown in Scheme 1.

It is known that azacycloheptatetraene **2f** and many of its derivatives absorb broadly around 350 nm.[7,9,12,13,28,31−33] These absorptions are seen in the spectra of **3f** in Figure 4 and in the spectra of 5-methyl-1-azacycloheptatetraene in Figures 7 and 10, which have been included for the sake of comparison. The TRIR experiments confirm that the disappearance of this broad absorption on the 100 μs time scale (seen in Figures 7 and 10), when **1a** is subjected to LFP, is, in fact, due to the rearrangement of **1f** to **9**.

**Reactions on the Nanosecond Time Scale.** It is clear from Figures 7, 8, and 9 that the carbazole, formed on the nanosecond time scale, does not come from **1f** ($\lambda_{max} \approx 350$ nm), but is produced from a precursor that absorbs in the visible region with a maximum at ∼430 nm. It is possible to write several structures that might be assigned to this precursor of **9**. Singlet nitrene **1b**, isocarbazole **4**, and tetracyclic aziridines **5** and **6** are all formal possibilities. However, the very high energies computed for **5** and **6** (Table 1) make them less plausible than **1b** and **4** as carriers of the transient absorption observed at 430 nm.

The spectra of most singlet arylnitrenes reveal strong absorption bands in the near UV region with maxima in the range of 320−405 nm.[9,13,28,31−33] However, it has been previously demonstrated[28,31] that ortho substituents can significantly influence the absorption spectra of singlet phenylnitrenes. Therefore,
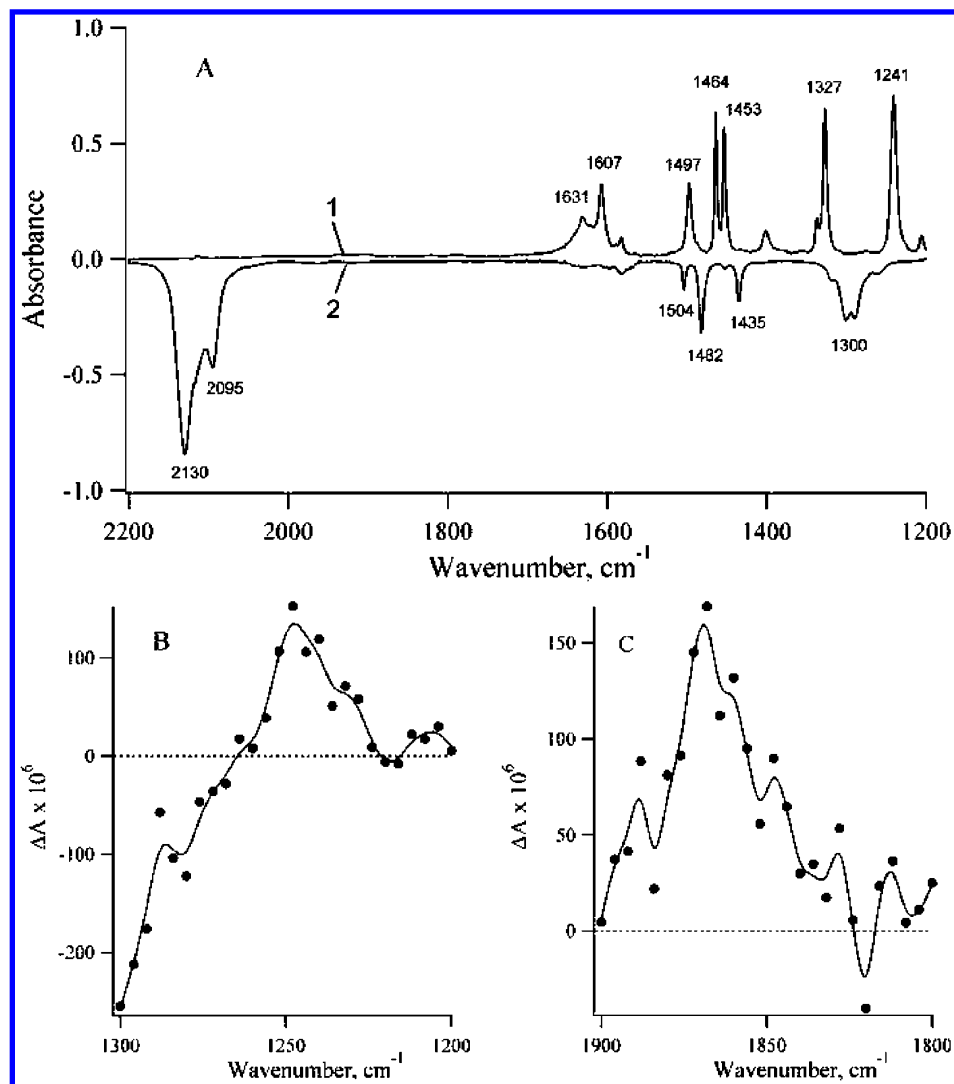
**Figure 11.** FT-IR spectra of (1) carbazole **9** and (2) *ortho*-biphenyl azide (**1a**) in acetonitrile-$d_3$ (A) and the TRIR spectra obtained after excitation of **1a** in acetonitrile at ambient temperature (B, C). Spectrum B, which was obtained by averaging over a time window of 350−450 μs, shows the 1200−1300 cm$^{-1}$ region of the spectrum, where **9** absorbs. Spectrum C, which was obtained by averaging over a time window of 0−2.5 μs, shows the 1800−1900 cm$^{-1}$ region of the spectrum, where **1f** absorbs.
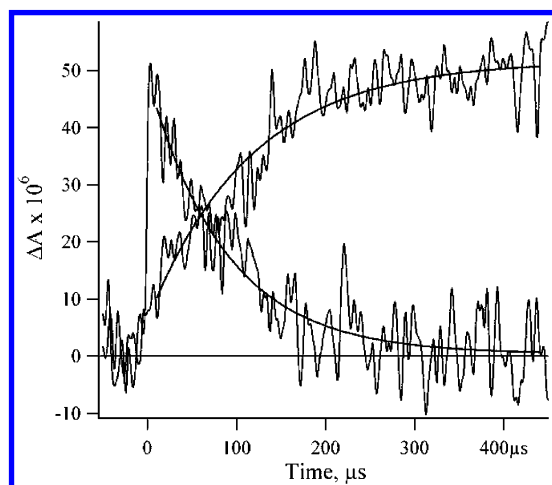


**Figure 12.** Kinetic traces for the growth of carbazole **9** (1241 cm$^{-1}$) and the decay of azacycloheptatetraene **1f** (1868 cm$^{-1}$), obtained by TRIR spectroscopy after LFP of **1a** in acetonitrile at ambient temperature.

the possibility that singlet nitrene **1b** is the carrier of the absorption band at 430 nm cannot be summarily dismissed.

Because singlet *ortho*-biphenylnitrene (**1b**) is predicted to have low barriers to cyclization to **1e** and **4**, LFP of azide **1a** was performed at 77 K, conditions which should "freeze out" nitrene cyclization and afford the best chance of direct observation of **1b**. LFP (266 nm) of **1a** in glassy 3-methylpentane at 77 K produces the spectra in Figure 13. The transient spectrum, recorded immediately after the flash (spectrum 1), has $\lambda_{max} = 410$ nm and decays with an observed rate constant of $(1.7 \pm 0.1) \times 10^7$ s$^{-1}$ ($\tau = 59 \pm 3$ ns). The decay of this species is accompanied by the growth ($k_{obs} = (1.6 \pm 0.1) \times 10^7$ s$^{-1}$) of an absorption, centered at 345 nm, with a weaker absorption at 400 nm and a shoulder at 320 nm (spectrum 2). The latter spectrum is identified as that of triplet *ortho*-biphenylnitrene (spectrum 3), which can be formed as a persistent species by continued irradiation of **1a** at 77 K. Thus, we conclude that singlet *ortho*-biphenylnitrene (**1b**) has been detected by LFP of **1a** at 77 K, has a $\lambda_{max} = 410$ nm, and relaxes cleanly to the lower energy triplet (**1c**) under these conditions.

LFP of perdeutero-2-biphenyl azide (**1a**-$d_9$) at 77 K again produces a transient that absorbs at 410 nm and has a lifetime of 80 ± 2 ns. The H$_9$/D$_9$ isotope effect on intersystem crossing
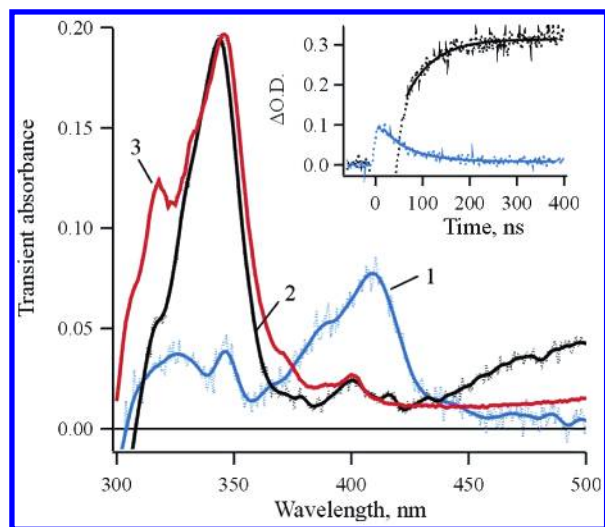
**Figure 13.** Transient absorption spectra detected over a window of 10 ns, following LFP of *ortho*-biphenyl azide (**1a**) in glassy 3-methylpentane at 77 K. Spectrum 1 was obtained just after the laser pulse and is assigned to singlet *ortho*-biphenylnitrene **1b**. Spectrum 2 was obtained 100 ns after the laser pulse and is assigned to triplet *ortho*-biphenylnitrene **1c**. Spectrum 3 was obtained after 10 s of irradiation of **1a** and corresponds to the spectrum of **1c**. The inset shows kinetic traces for the growth of **1c** and the decay of **1b**.

of **1b** to **1c** is thus $1.3 \pm 0.1$ at 77 K. The same results were obtained with either 266 or 308 nm excitation.

Because no other products were detected at 77 K, we can conclude that the rates of cyclization of **1b** must be much less than $1.7 \times 10^7$ s$^{-1}$ at this temperature. Assuming that the preexponential factor for cyclization is $10^{13}$ s$^{-1}$, we deduce that the barriers to singlet nitrene cyclization to **4** and **1e** are larger than 2 kcal/mol, provided that friction in the glass does not impede the rearrangement.

Singlet *ortho*-biphenylnitrene (**1b**) has an absorption band with a maximum at 410 nm, so we have assigned the transient absorption that has a maximum at 430 nm in solution (Figures 7–9) to isocarbazole **4**. To confirm this assignment, we studied the perdeutero analogue of **1a** (**1a**-$d_9$). Isocarbazole **4** isomerizes to **9** via a 1,5-hydrogen shift. Therefore, there should be an H/D kinetic isotope effect on the rate of disappearance of **4**.

LFP of **1a**-$d_9$ at ambient temperature produces spectra similar to those observed upon LFP of **1a** (Figure 7). As in the case of **1a**, the growth of carbazole absorption at 290 nm on the nanosecond time scale is accompanied by the decay of transient absorption in the visible region at 400–500 nm. The kinetics of growth and decay are shown in Figure 8B, and they can again be fit with an exponential function. The time constants of growth and decay are consistent with each other and equal to $240 \pm 10$ ns in pentane at ambient temperature. These time constants are a factor of $3.4 \pm 0.2$ slower than those for the growth and decay curves in Figure 8A. Therefore, a pronounced kinetic isotope effect on the reaction is observed, which is consistent with the reaction being the isomerization of isocarbazole **4** into carbazole **9** by a 1,5-hydrogen shift.

As shown in Figure 10, **4** is not detected upon LFP of **1a** in acetonitrile. We posit that trace quantities of water in acetonitrile catalyze the transformation of **4** into **9**. Indeed, methanol was also found to accelerate the disappearance of the transient absorption of **4** produced upon LFP of **1a** in pentane. The bimolecular rate constants, $k_{MeOH}$, for methanol catalysis of the

rearrangements of **4** and **4**-$d_9$ to **9** were determined to be $(6.9 \pm 0.7) \times 10^8$ and $(3.8 \pm 0.4) \times 10^8$ M$^{-1}$ s$^{-1}$, respectively, at ambient temperature. A reasonable mechanism for this catalysis is shown in eq 3.
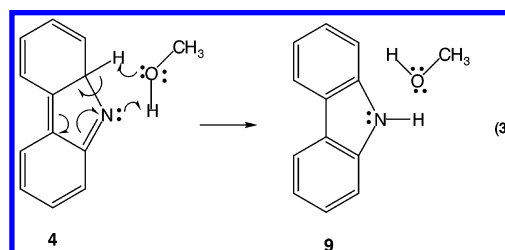


We studied the temperature dependence of the rate constants ($k_{1,5}$) for the decay of **4** and **4**-$d_9$ in pentane. Arrhenius treatment of these data is presented in Figure 14A. At temperatures greater than 220–250 K, the data follow the Arrhenius Law. However, the data deviate significantly from linearity below 220 K.[36]

It must be noted that the temperature dependencies in Figure 14A are very similar to those in Figure 5 for disappearance of singlet *para*-biphenylnitrene (**3b**). However, assignment of the transient absorbance at 430 nm to singlet *ortho*-biphenylnitrene **1b**, rather than to **4**, can be excluded, not only by the substantial isotope effect on the rate of disappearance of this absorption, but also its rate of disappearance at low temperatures.

For singlet nitrenes, the temperature dependence of the rate of disappearance can be described by eq 1 with the temperature-independent rate constant being that for intersystem crossing ($k_{isc}$).[9,13,28,31–33] If the temperature dependence of the rate constant for disappearance of the species absorbing at 430 nm is analyzed using eq 1, values of $k_{isc} = (5 \pm 1) \times 10^5$ and $(1.8 \pm 0.5) \times 10^5$ s$^{-1}$ are obtained in the LFP of **1a** and **1a**-$d_9$, respectively. However, the rate constants for intersystem crossing in **1b** and **1b**-$d_9$, measured at 77 K, were found to be much faster — $(1.7 \pm 0.1) \times 10^7$ and $(1.3 \pm 0.1) \times 10^7$ s$^{-1}$, respectively — and to show a much smaller isotope effect. Therefore, the temperature-independent rate constants for disappearance of the 430 nm absorption provide further evidence that singlet nitrene (**1b**) is not the carrier of this absorption.

**Benzazirine 1e.** Another interesting transient species was observed at 161 K (Figure 9). This species has a strong absorption band at ∼305 nm. Isocarbazole **4** is predicted to have strong absorptions at both 474 and 306 nm (Table 1). However, Figure 15 shows that, in Freon-113 at ambient temperature, the lifetime of the 305 nm transient absorption is only $12 \pm 2$ ns, which is about 6 times shorter than that for isocarbazole **4** disappearance or carbazole **9** formation. The observations of different decay rates for **4** and for the carrier of the transient absorption at 305 nm demonstrate that a reactive intermediate, other than **4**, must be responsible for the transient absorption at 305 nm in Figure 9.

---

(36) It is possible that this deviation from linearity involves a change in mechanism. For example, a 1,5-hydrogen shift at higher temperature might be replaced by a catalyzed process with not only a lower enthalpy of activation, but also with a much more negative entropy of activation. Alternatively, a contribution from tunneling to the 1,5-hydrogen shift reaction that forms **9** from **4** could be responsible for the deviation from linearity seen in Figure 14A. This interpretation has precedent in the work of Truhlar and co-workers.[37,38] Furthermore, Shizuka et al.[39] have reported experimental and theoretical evidence for tunneling during their study of a similar 1,5-hydrogen shift in the photorearranged intermediate formed from *N*-acetylpyrrole. However, the very small H/D kinetic isotope effect of less than 3 at low temperatures does not seem to be consistent with a mechanism involving temperature-independent tunneling below 220 K.
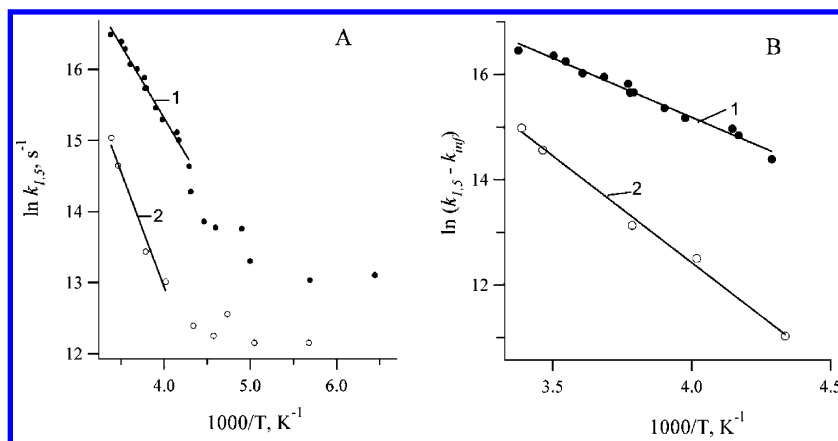
**Figure 14.** (A) Arrhenius treatment of the decay rate constant of isocarbazole **4** in pentane, measured after LFP of **1a** (1) and **1a**-$d_9$ (2). (B) Arrhenius treatment of the effective rate constant ($k_{1,5} - k_{inf}$), where $k_{inf}$ is the value of $k_{1,5}$ at a temperature range of 160−220 K.
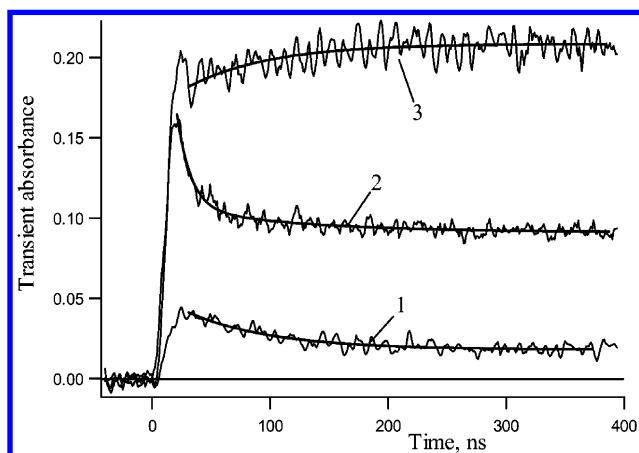


**Figure 15.** Changes in the transient absorption at (1) 440 nm, (2) 305 nm, and (3) 290 nm, detected after LFP of *ortho*-biphenyl azide **1a** in CF$_2$-ClCFCl$_2$ at ambient temperature.
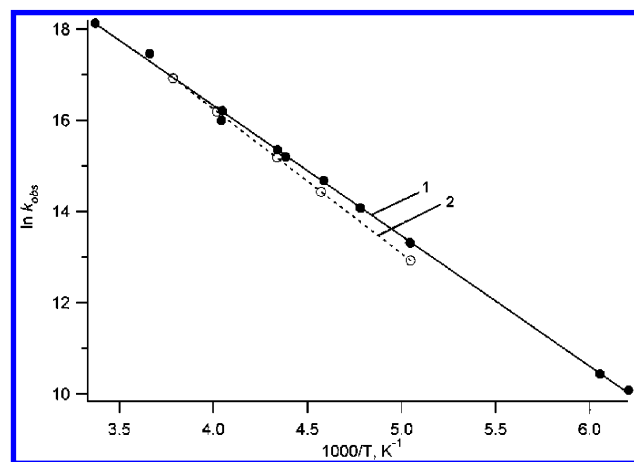


**Figure 16.** Arrhenius treatment of the observed rate constant ($k_{obs}$) for the disappearance of the transient species that absorbs at ~305 nm and is produced upon LFP of **1a** (1) and **1a**-$d_9$ (2) in pentane.

The temperature dependence of the observed rate constants ($k_{obs}$) for the decay of 305 nm transient absorption (Figure 16), produced by LFP of **1a** and **1a**-$d_9$, is totally different from those for the disappearance of isocarbazole **4** and **4**-$d_9$ (Figure 14). Moreover, the kinetic isotope effect (KIE) on $k_{obs}$, the rate constant for decay of the transient species that absorbs at 305 nm, is insignificant, whereas the KIE on the rate of disappearance of **4** is ca. 3. The magnitude of $k_{obs}$ ($\lambda = 305$ nm) decreases

exponentially with the temperature, so the Arrhenius plots of ln $k_{obs}$ versus $1/T$ in Figure 16 give straight lines with $E_a = 5.7 \pm 0.1$ kcal/mol and $A = 10^{12.1 \pm 0.1}$ s$^{-1}$ for the undeuterated compound and $E_a = 6.3 \pm 0.1$ kcal/mol and $A = 10^{12.6 \pm 0.1}$ s$^{-1}$ for the perdeuterated species. In contrast, the Arrhenius plots in Figure 14 for the transient species that absorbs at 430 nm are curved at low temperatures.

The short-lived 305 nm transient species cannot be attributed to singlet nitrene **1b**. The rate constant of $2.2 \times 10^4$ s$^{-1}$ for decay of the 305 nm transient species at even 160 K is much slower than $k_{isc} = 1.7 \times 10^7$ s$^{-1}$ for disappearance of **1b** and appearance of **1c** at 77 K. If the transient absorption at 305 nm were due to **1b**, the rate of disappearance of this absorption could be faster than or equal to, but never slower than, the rate of intersystem crossing to the triplet ground state of the nitrene (**1c**).

Other possible structures that might be assigned to the carrier of the transient absorption at 305 nm are benzazirine **1e** and tetracyclic aziridines **5** and **6**. The high energies (Table 1) computed for the latter two cyclization products of **1b** make them much less likely than **1e** to be the transient species observed at 305 nm. Consequently, the transient species that absorbs strongly at 305 nm is assigned to benzazirine **1e**.

The difference spectrum (Figure 9B) was obtained by subtracting the transient spectrum measured 4 $\mu$s after the laser flash from the spectrum measured 150 $\mu$s after the laser flash. The difference spectrum has two prominent negative peaks at 305 and 350 nm at 161 K. Both of these peaks correspond to the disappearance of benzazirine **1e** ($\tau = 41 \mu$s, 161 K), although we cannot exclude the possibility that triplet nitrene **1e** contributes to the peak at 350 nm.

Direct observations of benzazirines are rare. Other cases are the azirine produced by LFP of 2,4,6-tri-*tert*-butylphenyl azide in pentane at ambient temperature[40] and the matrix-isolated azirines, observed by IR and/or UV−vis spectroscopy, during the photolysis of 1-naphthyl azide,[41] 2,6-difluorophenyl azide,[42] and pentafluorophenyl azide[42] in argon at 10 K.

(37) Liu, Y.-P.; Lynch, G. C.; Truong, T. N.; Lu, D.-H.; Truhlar, D. G.; Garrett, B. C. *J. Am. Chem. Soc.* **1993**, *115*, 2408.
(38) Kim, Y.; Corchado, J. C.; Vill, J.; Xing, J.; Truhlar, D. G. *J. Chem. Phys.* **2000**, *112*, 2718.
(39) Kimura, Y.; Yamamoto, M.; Tobita, S.; Shizuka, H. *J. Phys. Chem. A* **1997**, *101*, 459.
(40) Tsao, M.-L.; Platz, M. S., unpublished results.
(41) Dunkin, I. R.; Thomson, P. C. P. *J. Chem. Soc., Chem. Commun.* **1980**, 499.
(42) Morawietz, J.; Sander, W. *J. Org. Chem.* **1996**, *61*, 4351.

Evidence that supports the assignment of **1e** as the carrier of the 305 nm absorption is provided by the results of our DFT calculations. Our TD-DFT calculations predict that **1e** will intensely absorb UV−vis light at 343 and 300 nm (Table 1, Figure 9B). This prediction is in reasonable agreement with the wavelengths of the transient absorptions in Figure 9B. Furthermore, our DFT calculations predict that the barrier to ring expansion of **1e** to **1f** is $\Delta H^{\ddagger} = 4.7$ kcal/mol (Figure 1), which is within 1 kcal/mol of the experimental value of $\Delta H^{\ddagger} = 5.7$ kcal/mol, obtained from the Arrhenius plot in Figure 16. As was already noted in Section II.1, the calculated barrier for ring opening of **1e** is 1.1 kcal/mol higher than the calculated barrier for ring expansion of the unsubstituted benzazirine (**2e**), and the higher barrier for ring expansion of **1e** to **1f** is what makes it possible to observe **1e** directly, before it undergoes ring opening to **1f**.

### III. Discussion

Our calculations predict and our experiments confirm that azacycloheptatetraene **1f** serves as the intermediate from which carbazole **9** is formed on the millisecond time scale. The observed rate constant for the formation of carbazole on the millisecond time scale, first reported by Berry and Sundberg and co-workers, has been found by our TRIR study to equal the observed rate constant for disappearance of **1f**. The rearrangement of ketenimine **1f** to **9** is a complicated function of the rate constants for the elementary reactions shown in Scheme 1. However, with some reasonable assumptions, it is possible to derive a simple expression for $k_{obs}$, the rate constant for formation of **9** from **1f**.

Our experiments find that rearrangement of **4** to **9** is very fast. Thus, it is reasonable to assume that formation of **4** is irreversible and, therefore, the rate constant of formation of **9** from **1f** is essentially the same as the rate constant of formation of **4** from **1f**. If the steady-state approximation is applied to singlet nitrene **1b**, azirine **1e**, and isocarbazole **4**, and if it is further assumed that **1e** undergoes ring opening to **1f** much faster than reversion to **1b** ($k_{ro} \gg k_{-c}$), eq 4 is obtained for $k_{obs}$.

$$k_{obs} = \frac{k_{-c}}{K_{ro}} \times \frac{k_{isc} + k_{car}}{k_c + k_{isc} + k_{car}} \qquad (4)$$

where the equilibrium constant $K_{ro} = k_{ro}/k_{-ro}$.

If cyclization of **1b** to **1e** is much faster than both intersystem crossing and cyclization of **1b** to **4** ($k_c \gg k_{isc} + k_{car}$), and if $k_{car} \gg k_{isc}$, which seems reasonable at ambient temperature, then eq 4 can be reduced to eq 5,

$$k_{obs} = \frac{k_{isc} + k_{car}}{K_{ro}K_c} = \frac{k_{car}}{K_{ro}K_c} \qquad (5)$$

where $K_c$ is the equilibrium constant for the cyclization reaction ($K_c = k_c/k_{-c}$). According to eq 5, the activation enthalpy for rearrangement of **1f** to **4** (and thence **9**) would then be the sum of the activation enthalpy for the cyclization of singlet *ortho*-biphenylnitrene **1b** to isocarbazole **4** and the overall enthalpy of isomerization of azacycloheptatetraene **1f** to singlet nitrene **1b**. Cyclization of **1b** to **4**, with rate constant $k_{car}$, would be the rate-determining step in the formation of both **4** and **9**.

On the other hand, if the rate constant of cyclization of **1b** to **4** is much faster than the rate constant of both intersystem

crossing and of cyclization of **1b** to **1e** ($k_{car} \gg k_{isc} + k_c$), eq 4 can be reduced to eq 6.

$$k_{obs} = \frac{k_{-c}}{K_{ro}} \qquad (6)$$

In this case, the activation enthalpy for formation of **4** would be the sum of the activation enthalpy for the reversion of azirine **1e** to singlet *ortho*-biphenylnitrene (**1b**) and of the enthalpy of the ring closure reaction of azacycloheptatetraene **1f** to azirine **1e**. The rate-determining step in the formation of both **4** and **9** would then be reversion of azirine **1e** to singlet nitrene **1b**, with rate constant $k_{-c}$.

However, if $k_{car}$ really were much larger than $k_c$, formation of **1f** would not have been observed in our LFP experiments, nor would Sundberg and co-workers[3] have isolated trapping products formed from **1f**. Thus, $k_{car}$ cannot be much bigger than $k_c$.

On the other hand, the Sundberg group showed[3] that even concentrated diethylamine, which efficiently traps **1f**, only partially suppresses the formation of carbazole. In fact, at high concentrations of diethylamine, comparable amounts of trapping product and **9** were isolated. Thus, we conclude that $k_c$ and $k_{car}$ must have comparable values, as was predicted by our CASPT2 calculations.

According to the B3LYP results in Figure 1, the rate-determining step in the formation of **4** from **1f** is passage over the TS that connects benzazirine **1e** to singlet nitrene **1b**. $\Delta H^{\ddagger}$ for this step is computed to be $24.8 - 11.6 = 13.2$ kcal/mol by B3LYP, but the CASPT2 energies in Figure 1 suggest a value that is 1.8 kcal/mol lower. Assuming a preexponential factor of $10^{13}$ s$^{-1}$, the rate constant of $k_{obs} = 10^4$ s$^{-1}$, obtained from our TRIR studies and also by the Sundberg group,[3c] gives $\Delta H^{\ddagger} = 11.8$ kcal/mol, in good agreement with the lower of the two calculated values.

We were not able to observe the kinetics of formation of **4** from **1b** at either ambient or low temperature (161 K). The rate constant for this process must be greater than $10^8$ s$^{-1}$, so the activation energy for this process must be very small. When one assumes that the preexponential factor for cyclization of singlet *ortho*-biphenylnitrene **1b** is $10^{13}$ s$^{-1}$, the activation energy must be less than 3.7 kcal/mol.

The CASPT2//CASSCF energy difference between singlet nitrene **1b** and the TS for its cyclization to **4** is 6.0 kcal/mol (Figure 1). Subtracting 2−3 kcal/mol, to correct for the overestimation of the energy barrier to arylnitrene cyclization at the CASPT2 level,[27] the barrier to cyclization of **1b** to form **4** is estimated to be 3−4 kcal/mol, which is consistent with the experimental result. The calculations predict and our experiments agree that the barrier to cyclization of **1b** is at least 2 kcal/mol lower than that for cyclization of unsubstituted phenylnitrene (**2b**).

At ambient temperature, the rates of formation of benzazirine **1e** and isocarbazole **4** in the LFP of *ortho*-biphenyl azide **1a** are too fast for us to measure. It is most economical to propose that all of the **1e** and **4** formed are in the reactions of relaxed singlet nitrene **1b**. Unfortunately, the possibility that some or all of the cyclization products **1e** and **4** are formed from an electronically or vibrationally excited state of the nitrene ($^1$**1b***) cannot be excluded. Possible evidence of the presence of this

complication is found in the dependence of the product ratio (carbazole/**1g**) on the excitation wavelength.[3b]

It can be seen in Figure 7 and in the data of Sundberg et al.[3c] that there is at least one additional intermediate formed in the photolysis of **1a** and that the lifetime for its decay is longer than that for azacycloheptatetraene (**1f**) decay and carbazole **9** formation from **1f** ($\tau = 1/k_{obs}$). According to our DFT calculations, **4** can undergo exothermic 1,5-hydrogen shifts to form not only carbazole **9**, but also isomeric isocarbazoles **7** and **8** (Figure 2). Both of these isocarbazoles are predicted to have an intense absorption around 360 nm (Table 1), and we propose that **7** and **8** are responsible for the longer lived, long-wavelength absorptions seen in Figure 7. Presumably, subsequent 1,5-shifts in **7** and **8** re-form **4** and eventually yield more carbazole **9**, seconds to minutes after the laser pulse. Catalysis of the rearrangements of **7** and **8** to **9** by adventitious water is likely to reduce the barrier heights for these reactions in solution from the 25−35 kcal/mol that is computed for these reactions in the gas phase.

## IV. Conclusions

Laser flash photolysis (LFP, 266 nm, 5 ns) of *ortho*-biphenyl azide **1a** in glassy 3-methylpentane produces singlet *ortho*-biphenylnitrene **1b** ($\lambda_{max} = 410$ nm, $\tau = 59$ ns), which at 77 K cleanly relaxes to the lower energy triplet nitrene **1c** ($\lambda_{max} = 340$ nm). The triplet nitrene is persistent in the glass. LFP of **1a** at higher temperatures in fluid solution does not produce singlet nitrene **1b** as a detectable species on the nanosecond time scale. Instead, benzazirine **1e** and isocarbazole **4** are formed almost immediately after the laser pulse.

Benzazirine **1e** ($\lambda_{max} = 305$ nm) has a lifetime of 12 ns in Freon-113 and rearranges to azacycloheptatetraene **1f** ($\lambda_{max} = 350$ nm), which was identified via TRIR spectroscopy by its characteristic ketenimine absorption at 1868 cm$^{-1}$. This compound serves as a reservoir for singlet nitrene **1b**, and cyclization of **1b** to isocarbazole **4** produces carbazole **9** on the millisecond time scale. The rate of disappearance of **1f** ($8.3 \times 10^3$ s$^{-1}$) is equal, within experimental error, to the rate of appearance of carbazole **9** ($11 \times 10^3$ s$^{-1}$) on this time scale.

Isocarbazole **4** ($\lambda_{max} = 430$ nm) isomerizes to carbazole **9** ($\lambda_{max} = 290$ nm) with a lifetime of 70 ns in pentane at ambient temperature. The rate of decay of the absorption due to **4** is equal to the rate of the growth of the absorption due to **9** on the nanosecond time scale. Isocarbazole-$d_9$ has a lifetime of 240 ns under these conditions. The kinetic isotope effect is due to isomerization of isocarbazole **4** to **9** by a 1,5-hydrogen shift, which is catalyzed by water and methanol. One or both of the two other isocarbazoles (**7** and **8**) that can be formed from **4** by 1,5-hydrogen shifts have been detected by their long-wavelength absorptions.

Throughout this study, the UV absorptions, predicted by TD-DFT calculations and shown in Table 1, were very helpful in identifying each of the reactive intermediates, formed in the LFP of **1a**. In addition, the relative energies, predicted by the B3LYP and CASPT2 calculations and summarized in Figures 1 and 2, are in excellent agreement with those obtained from the results of our experiments.

Particularly noteworthy is the experimental finding, both in this spectroscopic study and in Sundberg's chemical trapping experiments,[3] that closure of singlet nitrene **1b** to benzazirine **1e** is highly competitive with the more thermodynamically favorable closure of **1b** to isocarbazole **4**. This experimental finding is predicted by CASPT2 but not by UB3LYP.

The failure of the UB3LYP calculations to predict correctly the relative energies of the TSs leading from **1b** to **1e** and **4** can be attributed to the different amounts of spin contamination in the wave functions for the two TSs. This failure cautions against the use of UB3LYP calculations, not only for open-shell singlet diradicals (e.g., **1b**), but also for TSs that have significant amounts of open-shell singlet character.

## V. Experimental Section

**Materials.** The syntheses of *ortho*-, *ortho*-$d_9$, and *para*-biphenyl azides from their amino analogues followed published procedures.[1,3] *ortho*-Aminobiphenyl-$d_9$ was obtained from CDN Isotopes, Inc.

**Laser Flash Photolysis Apparatus.** The current design of the flash photolysis instrument is based upon the previously described instrument[43] with the following changes. The older version of the instrument used a hard-wired computer interface. The upgrade of this basic design is software centered, using the LabView graphic programming language, which allows for greater ease in the optimization, integration, and use of the instrument. The new version employs a single ARC SP-308 monochromator/spectrograph, with 1-015-300 grating. This model features dual ports, one with a slit and a photomultiplier[43] for kinetic measurements and the other with a flat field and a Roper ICCD-Max 512T Digital ICCD camera for spectroscopic measurements, with up to 2 ns temporal resolution. The single monochromator/spectrograph negates the need for separate optimization of kinetic and spectral measurement system alignment, thus facilitating the usage of both types of measurements. The ICCD controller is directly interfaced to the computer using the Roper WinView software and ST-133A controller.

Kinetic data acquisition uses a Tektronix TDS 680C 5 Gs/s 1 GHz oscilloscope directly interfaced via a National PCI-GPIB to the Columbus Microsystems 400 MHz Pentium II computer running a custom LabView control and acquisition program. The laser, arc lamp, shutter, and other timing and control signals are routed through a National PCI-6602 DAQ interface. The excitation of the samples was provided by a Spectra Physics LAB-150-10 (~5 ns) water-cooled laser, which was configured to supply 266 nm radiation. The measurement beam is supplied by a PTI 150 W xenon arc lamp with a LPS 210 power supply, LPS 221 stand alone igniter, A-500 compact arc lamp housing, and MCP-2010 pulser, which allows for controlled pulsing of the arc lamp, with pulses 0.5−2.0 ms in duration and up to 160 A in amplitude.

Temperature was maintained at 77 K by means of boiling liquid nitrogen or varied in the range of 160−300 K and kept to within ±1 K by passing a thermostabilized nitrogen stream over the sample. In these experiments, a quartz cuvette was placed in a quartz cryostat.[32] The sample solutions were changed after every laser shot, unless otherwise indicated.

**Time-Resolved Infrared (TRIR) Studies.** TRIR experiments were conducted with a JASCO TRIR-1000 dispersive-type IR spectrometer with 16 cm$^{-1}$ resolution, following the method described in the literature.[44−46] Briefly, a reservoir of sample solution (10 mL of a 4 mM solution of 2-biphenyl azide) was continually circulated between two calcium fluoride salt plates with a 0.5 mm path length. The sample

(43) Gritsan, N. P.; Zhai, H. B.; Yuzawa, T.; Karweik, D.; Brooke, J.; Platz, M. S. *J. Phys. Chem. A* **1997**, *101*, 2833.
(44) (a) Yuzawa, T.; Kato, C.; George, M. W.; Hamaguchi, H. *Appl. Spectrosc.* **1994**, *48*, 684. (b) Iwata, K.; Hamaguchi, H. *Appl. Spectrosc.* **1990**, *44*, 1431.
(45) Toscano, J. P. *Adv. Photochem.* **2001**, *26*, 41.
(46) For recent reviews, see: (a) Ford, P. C.; Bridgewater, J. S.; Lee, B. *Photochem. Photobiol.* **1997**, *65*, 57. (b) Schoonover, J. R.; Strouse, G. F. *Chem. Rev.* **1998**, *98*, 1335. (c) George, M. W.; Turner, J. J. *Coord. Chem. Rev.* **1998**, *177*, 201. (d) George, M. W.; Poliakoff, M.; Turner, J. J. *Analyst* **1994**, *119*, 551.

was excited with a Coherent Infinity XPO/OPO Nd:YAG laser (266 nm, 40 Hz repetition rate, 0.5–0.6 mJ/pulse). The laser beam is crossed with the broadband output of a $MoSi_2$ IR source (JASCO). The intensity change of the IR light induced by photoexcitation is monitored as a function of time by an MCT photovoltaic IR detector (Kolmar Technologies, KMPV11-1-J1) with a 50 ns rise time, amplified by a low noise NF Electronic Instruments 5307 differential amplifier, and digitized by a Tektronix TDS784D oscilloscope. The TRIR spectrum is analyzed by the IGOR PRO program (Wavematrics Inc.) in the form of a difference spectrum, $\Delta A_t = -\log(1 + \Delta I_t/I)$, where $\Delta I_t$ is the intensity change induced by photoreaction at time $t$, and $I$ is the IR intensity of the sample without photoexcitation. Thus, depletion of reactant and formation of transient intermediates or products led to negative and positive signals, respectively.

**Supporting Information Available:** Figure S1: Transient absorption spectra of singlet (**3b**) and triplet (**3c**) *para*-biphenylnitrene produced upon LFP of *para*-biphenyl azide (**3a**) in glassy 3-methylpentane at 77 K. Computational data including optimized geometries, energies, thermal corrections, and IR frequencies for **1b**, **1c**, **1e**, **1e′**, **1f**, **1f′**, and **4**–**9** and corresponding transition structures, with TD-DFT electronic excitation wavelengths and oscillator strengths for **1c**, **1e**, **1e′**, **1f**, **1f′**, and **4**–**9** (PDF). This material is available free of charge via the Internet at http://pubs.acs.org.

JA0351591